



HAL
open science

VOC-free Synthesis of Waterborne Poly(hydroxy urethane)-(meth)Acrylics Hybrids by Miniemulsion Polymerization

Boris Bizet, Etienne Grau, Henri Cramail, José Maria Asua

► **To cite this version:**

Boris Bizet, Etienne Grau, Henri Cramail, José Maria Asua. VOC-free Synthesis of Waterborne Poly(hydroxy urethane)-(meth)Acrylics Hybrids by Miniemulsion Polymerization. ACS Applied Polymer Materials, In press, 10.1021/acsapm.0c00657 . hal-02920358

HAL Id: hal-02920358

<https://hal.science/hal-02920358>

Submitted on 24 Aug 2020

HAL is a multi-disciplinary open access archive for the deposit and dissemination of scientific research documents, whether they are published or not. The documents may come from teaching and research institutions in France or abroad, or from public or private research centers.

L'archive ouverte pluridisciplinaire **HAL**, est destinée au dépôt et à la diffusion de documents scientifiques de niveau recherche, publiés ou non, émanant des établissements d'enseignement et de recherche français ou étrangers, des laboratoires publics ou privés.

VOC-free Synthesis of Waterborne Poly(hydroxy urethane)-(meth)Acrylics Hybrids by Miniemulsion Polymerization

*Boris Bizet,^{ab} Etienne Grau,^a Henri Cramail^{*a} and José M. Asua^{*b}*

^a University of Bordeaux, CNRS, Bordeaux INP - LCPO, UMR 5629 - 16, avenue Pey Berland, F-33600, Pessac, France

^b POLYMAT, University of the Basque Country UPV/EHU, Joxe Mari Korta Center, Avenida Tolosa 72, 20018 Donostia-San Sebastián, Spain

KEYWORDS: Poly(Hydroxy)urethanes – PHUs, Bio-based Polymers, PU-Acrylic Hybrid, Miniemulsion, Coatings, NIPUs

ABSTRACT

A VOC-free method for the synthesis of Poly(hydroxyurethane)-(meth)acrylic waterborne hybrid dispersions was developed. Poly(hydroxyurethane)s (PHU) synthesized by bulk aminolysis of cyclic-carbonate derivatives using bio-sourced vegetable oil-based diamines was dissolved in (meth)acrylate monomers, the solution dispersed in water and polymerized in miniemulsion. Hybrid particles exhibiting core-shell morphology with the PHU in the shell were obtained. The performance of the

coating cast from these dispersions was studied, finding that by simply varying the PHU content and the casting conditions, widely different mechanical properties of PHU-(meth)acrylic hybrids could be obtained. The versatility of the synthetic method that is not limited to the type of (meth)acrylic monomers, opens the way for obtaining a broad range of environmentally friendly VOC and isocyanate free waterborne urethane-acrylic coatings and adhesives.

1. Introduction

Accessing high performance polymer materials with satisfactory properties and balanced production cost usually requires the synergistic combination of polymers with different and even antagonist properties. Hybrids of polyurethanes (PU) and (meth)acrylic polymers are one of these synergistic combinations. PUs provide superior mechanical properties such as toughness, flexibility and abrasion resistance,¹⁻⁴ whereas poly(meth)acrylics are affording materials with good outdoor and alkali resistance, as well as pigment compatibility.⁴⁻⁶ PU-(meth)acrylic hybrids are often prepared as waterborne dispersions that find applications as coatings and adhesives. The field has been recently reviewed aiming at establishing the link between synthesis, structure and properties.⁷ The final outlook of that review points out the challenges created by the environmental impacts of both the raw materials used in the synthesis and the need of developing low volatile organic compound (VOC) and preferably VOC-free synthetic routes. Currently, di-isocyanates are used in the PU synthesis, but they may cause health issues such as asthma, dermatitis and even poisoning.⁸⁻¹⁰ In addition, isocyanates require the use of phosgene in their synthesis, which is a highly toxic gas that can cause death by inhalation. Solvent free PU-(meth)acrylic hybrids have been obtained by synthesizing the PU prepolymer using a mixture of (meth)acrylic monomers as diluents and then

dispersing the solution in water.¹¹⁻¹⁷ However, achieving good colloidal stability is challenging and requires fine tuning of the synthetic approach.¹⁸

This study addresses the challenge of synthesizing isocyanate-free, solvent-free waterborne PU-(meth)acrylic dispersions. To the best of our knowledge, there are only two publications related to waterborne Non Isocyanate Polyurethane (NIPU)-acrylic dispersions.^{19,20} In these previous studies, monofunctional urethane methacrylates (UMA) were prepared by aminolysis of ethylene carbonate and aliphatic amines in methylene chloride and then the resulting product was functionalized with methacrylic anhydride in DMF. The UMAs were copolymerized with methyl methacrylate (MMA)/Butyl Acrylate (BA) in a seeded emulsion polymerization. The method presents some drawbacks as it involves several steps and uses solvents. Furthermore, the hybrids do not contain poly(urethane) chains, but single urethane moieties pendant from the (meth)acrylic backbone.

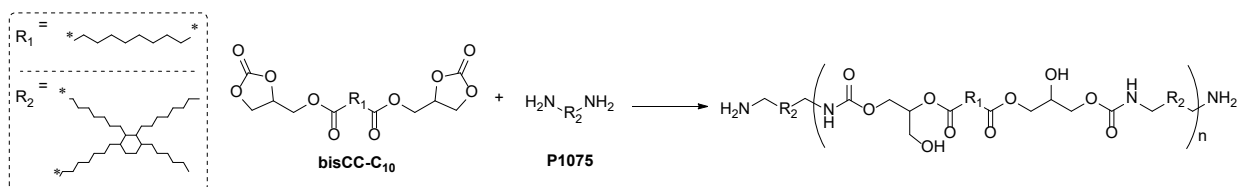
In order to overcome these drawbacks, two complementary strategies were explored in this study. The first one involved the formation of the isocyanate-free polyurethane by aminolysis of cyclic-carbonate derivatives using (meth)acrylic monomers as reacting media. This process leads to poly(hydroxy urethane)s – often called PHU.²¹⁻²³ The idea was to disperse the PHU/(meth)acrylates solution in water through a miniemulsification process, and then to polymerize the (meth)acrylic monomers by free radical polymerization. The second strategy explored was (i) to form the PHUs by bulk aminolysis of cyclic-carbonate derivatives using bio-sourced vegetable oil-based diamines and (ii) to dissolve the PHU in (meth)acrylate monomers, the mixture serving as the organic phase of a miniemulsion. Subsequent polymerization of the (meth)acrylic monomers leads to the hybrid PU/(meth)acrylates waterborne dispersion. The performance of the films cast from the hybrid waterborne dispersions was finally studied.

2. Results and Discussion

2.1. First strategy: solution polymerization in a (meth)acrylic solvent

As explained in the introduction, the first strategy involves the polymerization of cyclic carbonates with diamines in (meth)acrylic monomers, followed by dispersion in water and subsequent free radical polymerization of the (meth)acrylates.

As amines can potentially react with acrylic monomers, typically in an *aza*-Michael-type mechanism, the occurrence of this reaction was checked in the aminolysis reaction between a sebacic acid-derived bis-cyclic carbonate (bisCC-C₁₀) and the commercially available fatty-acid dimer diamine Priamine® 1075 (P1075) in Butyl Acrylate (BA) and Butyl Methacrylate (BMA) – Scheme 1.



Scheme 1. PHU pre-polymer utilized for the synthesis of PHU-Acrylics hybrid materials

It was found that BA suffered a significant reaction with the amine (Supporting Information – Figures S2 to S5). This is a strong drawback because side reactions consuming diamines will modify the stoichiometry substantially, thus reducing the polymer molar mass formed by this step-growth polymerization. Although BMA was only slightly affected by this reaction (Supporting Information – Figures S6-S7), the solubility of the monomer was low (Table S1) and therefore the strategy based on the

formation of PHU in (meth)acrylates was abandoned and efforts were concentrated on the second strategy, that involved the formation of the PHUs by bulk aminolysis of bis-cyclic-carbonate derivatives using a bio-sourced vegetable oil-based diamine followed by dissolution of the PHUs in (meth)acrylic monomers, then dispersion in water to form a miniemulsion and free radical polymerization of the vinylic monomers. Miniemulsion polymerization – even if limited in terms of industrial implementation – was performed because this process is particularly well suited for the synthesis of hybrid dispersions, especially when they involve the use of pre-polymers.^{24,25}

2.2. Second strategy: Bulk formation of the PHU prior to incorporation into a (meth)acrylic solvent

In this strategy, poly(hydroxy)urethanes (PHUs) were again synthesized through the aminolysis reaction between bisCC-C₁₀ and P1075 (Scheme 1). The stoichiometric ratio for the reactive moieties was used to target high molar masses according to Carother's theory.²⁶ The reactions were performed in bulk at 90°C for 24h. A necessary condition for the implementation of this approach is that the PHU should be soluble in the (meth)acrylates. Therefore, the solubility of the PHUs obtained with bisCC-C₁₀ and a series of diamines in butyl methacrylate (BMA) was determined. Table S2 shows that the solubility of the PHU strongly depended on its composition and a minimum amount of P1075 was needed to have a significant solubility in BMA. PHUs prepared using P1075 as the only diamine showed high solubility in BMA (up to 50 wt% at 80°C, Table S3).

The P1075-based PHU was dissolved in a mixture of BMA and stearyl acrylate (SA, costabilizer used to minimize Ostwald ripening²⁷) and miniemulsified in a solution of Dowfax 2A1 in deionized water using sonication (details in the experimental section). 40 wt% solids content miniemulsions were formed. They were polymerized using both

thermal oil-soluble initiators (2,2'-azobis(2-methylpropionitrile), AIBN, and benzoyl peroxide, BPO) as well as a water-soluble redox initiator (Tert-butyl hydroperoxide / ascorbic acid, TBHP/AsAc). A preliminary study showed that the oil-soluble thermal initiators (AIBN and BPO) yielded unsatisfactory results in terms of kinetics or extent for coagulation (details in Supporting Information). Therefore, the TBHP/AsAc redox system was preferred. Table 1 summarizes the reactions carried out (details are given in Supporting Information). The PHU was obtained by bulk polymerization of bisCC-C₁₀ and P1075 as described above. The oil phase of the miniemulsion was a mixture of PHU, BMA, SA and TBHP. It is worth pointing out that TBHP do not suffer any significant decomposition at temperatures below 90°C (half life time = 520h at 130°C),²⁸ and therefore can be safely mixed with the monomers. Several PHU contents (0 wt.%, 10 wt.%, 20 wt.% and 30 wt.%) were used. The organic phase was mixed with an aqueous solution of Dowfax 2A1 under strong magnetic agitation and then sonicated. After sonication, an additional amount of Dowfax 2A1 was added to post-stabilize the miniemulsion. The reason for this post-stabilization step is due to the fact that when the viscosity of the organic phase is relatively low as it is the case here, the droplet size is determined by the availability of the surfactant and the surface concentration of the surfactant is just enough to provide stability, *i.e.*, the droplets are at their stability limit.²⁹ This situation often leads to stability problems during polymerization. Therefore, a useful strategy is to use a fraction of surfactant during miniemulsification and reserve a part to stabilize the droplets afterwards. The polymerizations were carried out at 70°C feeding semi-continuously an aqueous solution of AsAc. Different feeding times were used (2, 2.5 and 3 hours).

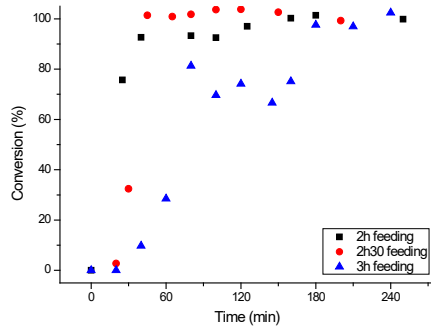
Table 1. Summary of the miniemulsion polymerizations

		Composition			
Basic recipe	PHU	0-30	wt%	} 96wt%	40 wt.% solids
	BMA	100-70	wt%		
	SA	4	wt%		
	Dowfax™ 2A1	1	wt% (wbo)		
	Water				
Post- Stabilization	Dowfax™ 2A1	1	wt% (wbo)		
	Water	< 1g			
Initiation	TBHP	0.05	wt% (wbo)		
	AsAc	0.05	wt% (wbo)		
	Water	<1g			

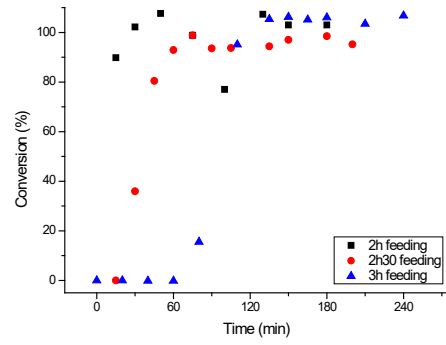
Figure 1 presents the variation of the gravimetric conversion (BMA) as a function of time during the miniemulsion polymerizations carried out with different PHU contents for three AsAc feeding times. Figure 2 presents the variations as a function of time of the particle diameter measured by DLS.

Figure 1 shows that, in all the cases, conversions close to 100% were obtained at the end of the process, although an induction period was observed. The reason was that the concentration of AsAc was low at the beginning of the process and the radicals generated were consumed by the inhibitor contained by the monomers (technical monomers were used). In general, the slower the feed rate of AsAc (longer feeding times), the longer the inhibition period. The inhibition period could also be reduced by increasing the flushing time as it is demonstrated in the experiments carried out with 30 wt% of PHU. Indeed, the inhibition time observed for the reaction where the AsAc was fed for of 2.5 hours was shorter than the inhibition observed with faster AsAc feeding (2 h) because a longer flushing time was used in the former experiment (90 min for the 2.5 h feeding vs. 60 min for the 2h one). When the inhibition was overcome, polymerization was fast in most cases.

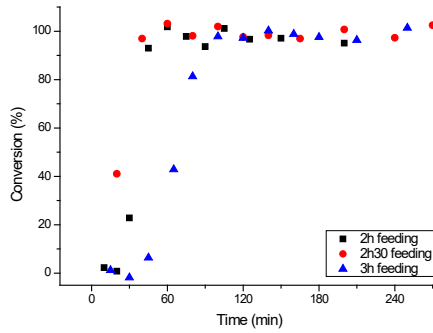
a)



b)



c)



d)

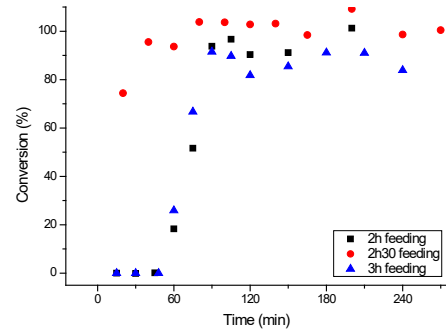


Figure 1. Effect of the AsAc feeding rate on the monomer conversion, obtained by gravimetry for different PHU contents, as a function of time. (a) 0 wt.% PHU, b) 10 wt.% PHU, c) 20 wt.% PHU, d) 30 wt.% PHU).

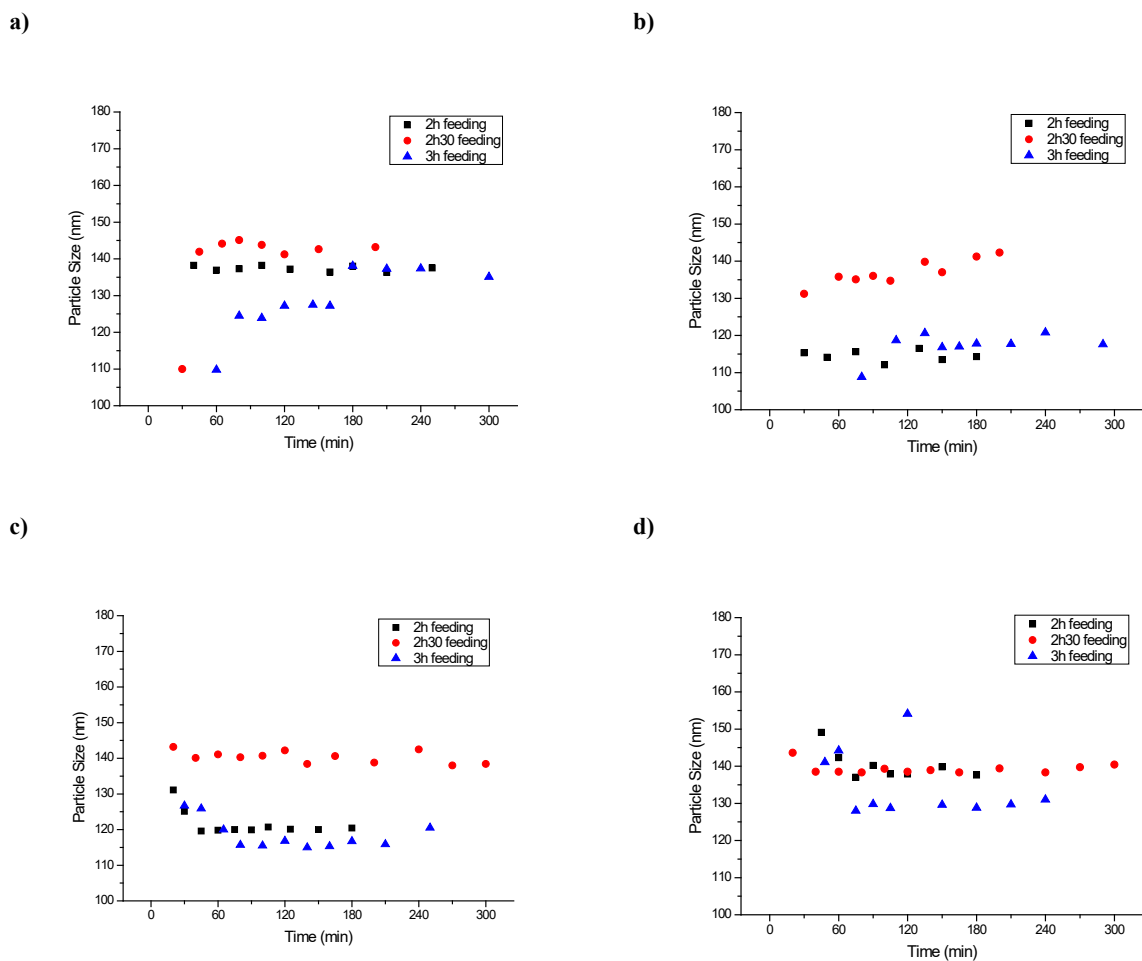


Figure 2. Variation of the particle size as a function of time (a) 0 wt.% PHU, b) 10 wt.% PHU, c) 20 wt.% PHU, d) 30 wt.% PHU).

For the experiments carried out with PHU, Figure 2 shows that particle size was roughly constant during the whole process, which is a characteristic of efficiently nucleated well stabilized miniemulsions. The reason is that if the miniemulsion is stable, initially the size of the monomer droplets is determined by DLS and, later, the monomer swollen polymer particles are measured. As the difference in volume between monomer droplets and monomer-swollen particles is only due to a density difference that is small, the differences in diameter are negligible. Figure 2 shows that the particle sizes obtained with 10 and 20 wt% of PHU, for an AsAc feeding time of 2.5 h, were larger in comparison to other cases. For efficiently nucleated stable miniemulsions, this effect can only be the result of the

differences in miniemulsion droplets. It has been demonstrated that miniemulsification by sonication is very sensitive to small details such as the geometry of the system, the position of the sonication tip and the flow patterns created by agitation in the flask.³⁰ Therefore, the observed deviations might be the result of inadvertent changes during miniemulsification. In the absence of PHU, the particle size substantially increased during the process, which suggests that SA was not able to form a stable miniemulsion. Indeed, it has been demonstrated that the presence of polymer reinforces the effect of the costabilizer²⁷ and therefore the polymerization likely occurred through a mixed emulsion-mini-emulsion mechanism. The processes were basically coagulum-free (Table 2). It is worth pointing out that unlike the first strategy, this method has basically no restrictions in terms of the (meth)acrylate monomers that can be used, and therefore can be employed to synthesize both coatings and adhesives.

Table 2. Characteristics of the synthesized latexes while investigating the use of redox radical initiators

% PHU [wt%]	PHU			Feeding time [h]	Coagulation [wt%]	Particle Size ^b [nm]	Hybrids			T _g ^d	MFFT [°C]
	M _n ^a [g.mol ⁻¹]	M _w ^a [g.mol ⁻¹]	Đ ^a				M _n ^c [kg.mol ⁻¹]	M _w ^c [kg.mol ⁻¹]	Đ ^c		
0 wt%	-	-	-	2h00	2.3	137	-	-	-	-	-
	-	-	-	2h30	0.9	143	2410	4220	1.7	29	30
	-	-	-	3h00	1.6	137	-	-	-	-	-
10 wt%	-	-	-	2h00	1.8	115	-	-	-	-	-
	21600	43000	2.0	2h30	1.8	142	2480	3780	1.5	-21/28	24
	-	-	-	3h00	1.8	117	-	-	-	-	-
20 wt%*	-	-	-	2h00	1.0	120	-	-	-	-	-
	21700	41100	1.9	2h30	2.1	138	2190	3280	1.5	-20/24	15
	-	-	-	3h00	1.8	116	-	-	-	-	-
30 wt%*	-	-	-	2h00	2.8	138	-	-	-	-	-
	21700	41100	1.9	2h30	4.3	140	2070	3170	1.5	-20/34	< 7
	-	-	-	3h00	1.6	131	-	-	-	-	-

^a Determined by SEC in DMF, with LiBr salts, PS calibration

^b Measured by DLS

^c Determined by SEC/MALLS. Because no LS signal was observed for the low molar mass peak (corresponding to the PHU), only the molar mass corresponding to the poly(BMA-co-SA), which had a LS signal, is reported

^d Measured by DSC of the dried films, 1st heating ramp (10°C/min)

-: not determined

*: the same PHU was used in the preparation of these latexes

SEC/MALLS analyses showed bimodal distributions when PHU was incorporated into the formulation, the low molar mass corresponding to the PHU – (Figure S11). Interestingly, the amount of PHU incorporated into the formulation did not seem to dramatically affect the final molar mass of the acrylic polymer; all values of M_w were in the range $2.10^6 - 2.5.10^6 \text{ g.mol}^{-1}$. It may be observed a trend showing that for the same feed rate of AsAc, the higher the PHU fraction, the lower the molar mass of polyBMA. This is due to the fact that, for similar particle sizes and for the same feed rate of AsAc, the frequency of radical entry in the particles was similar and hence the polymer chains grow a similar time. Under these conditions, the chain length is proportional to the monomer concentration in the particles that decreased as the PHU content increased.

Table 2 also presents the glass transition temperatures obtained by DSC (Figure S12). It can be seen that the T_g s of both phases were clearly observed and that the values were not affected by the PHU content, which indicates a neat phase separation. In this hybrid, the PHU was the softer phase and polyBMA the harder one. Therefore, the PHU content affected the minimum film forming temperature (MFFT). Table 2 shows that MFFT significantly decreased as the content of the soft PHU increased. This is an interesting characteristic, because by varying the T_g of the (meth)acrylic polymer and the fraction of the PHU, one can obtain a portfolio of waterborne coatings showing a wide range of properties.

The decrease in MFFT with the PHU content suggests that the PHU was located at the outer part of the particles and therefore participating in the formation of the film. Particle morphology was studied by TEM using phosphotungstic acid (PTA) as selective negative staining agent of the PHU. The TEM images are presented in Figure 3. It can be seen that the shell could only be observed for the highest PHU content (30 wt.%), For smaller contents the shell was too thin to be observed. Nevertheless, the image for 30 wt.% of

PHU clearly showed that core-shell particles were formed and that, in agreement with the hypothesis based on MFFT measurements, the shell was made out of PHU. The fact that the PHU is placed at the shell of the particles explains the strong effect of the PHU content on the MFFT (Table 2). This enables good film formation without the need of coalescing agents.

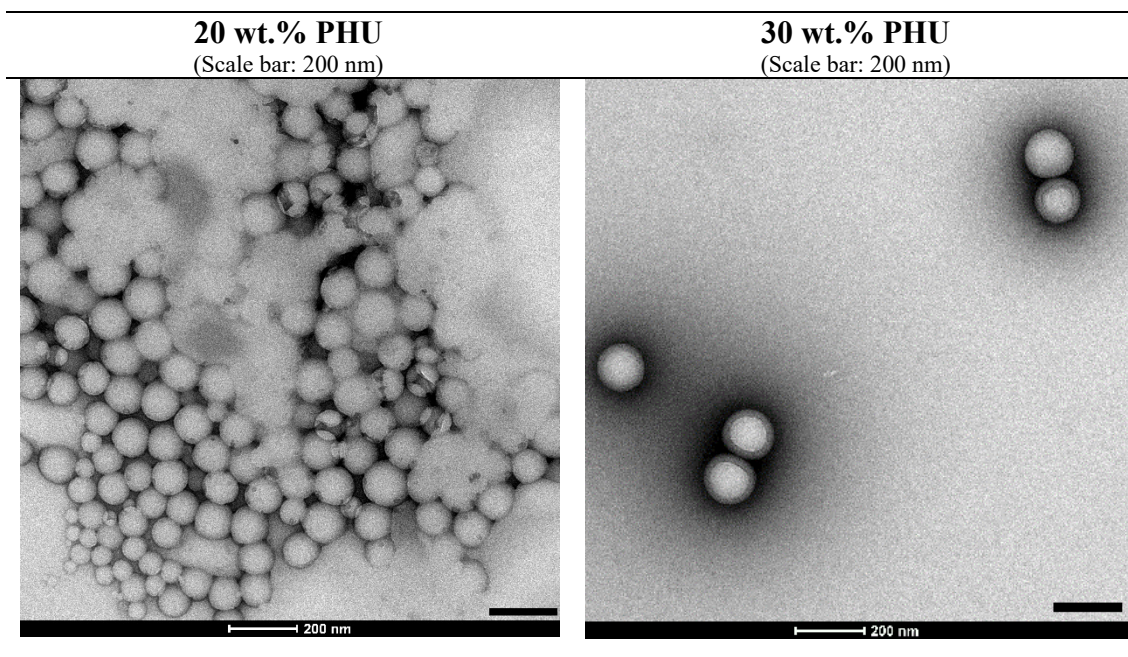


Figure 3. TEM images of the polymer particles for the latexes containing 20 wt.% PHU (left) and 30 wt.% PHU (right) formed with 2h30 feeding of AsAc.

Figure 4 shows that, in all cases, transparent films were obtained at 30 °C. This indicates that good quality of particle packing was achieved during the film formation process, perhaps due to the fact that the casting temperature was equal or higher than the MFFTs. Yellowing of the films could also be noticed in the case of PHU loadings higher or equal than 20 wt.%.

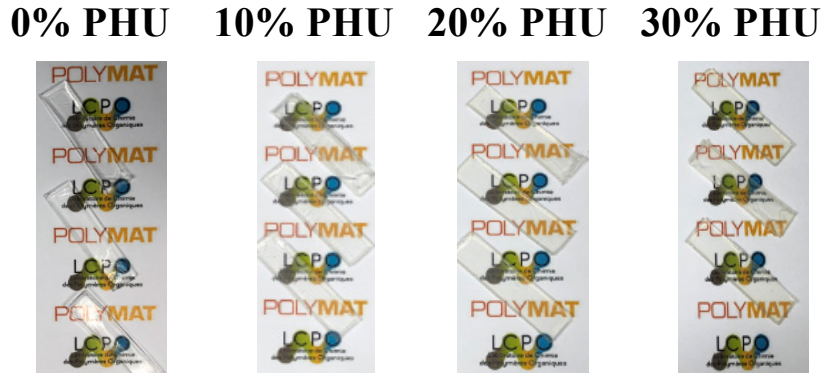


Figure 4. Pictures of the cast films at 30°C with different loadings of PHU.

Figure 5 presents the effect of the PHU content on the stress-strain curves. This figure also includes the effect of the casting temperature and thermal treatment for the 20 wt% PHU hybrid. Table 3 summarizes the effect of these variables on the Young's modulus, strain and stress at break and toughness.

It can be seen that, at 30°C, increasing the PHU content led to a softer material with a clear decrease of both Young's modulus and the stress at break as well as an increase of the strain at break. On the other hand, the effect of the casting temperature is more complex. When the films were cast at 45°C, Young's modulus and, in particular, the strain at break increased with respect to the film cast at 30°C, leading to a substantial increase in toughness. However, further increase of the casting temperature led to a decrease in Young's modulus, strain at break and toughness.

Complex effects of the casting temperature and thermal treatments on mechanical properties have been reported for other hybrid systems^{31–34} and have been explained by the modifications in the film morphology. Therefore, in order to investigate if this was the case in the present system, the morphology of the films was determined by TEM.

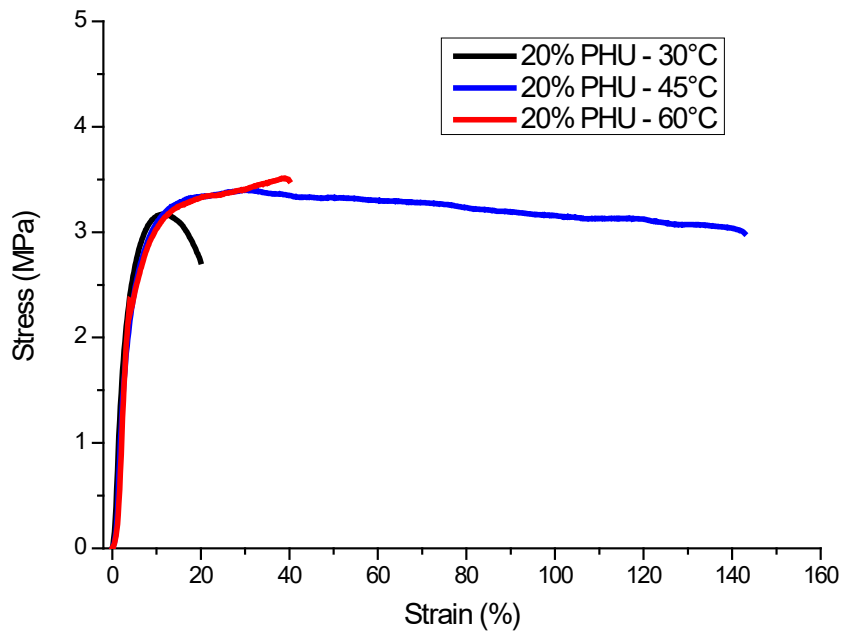
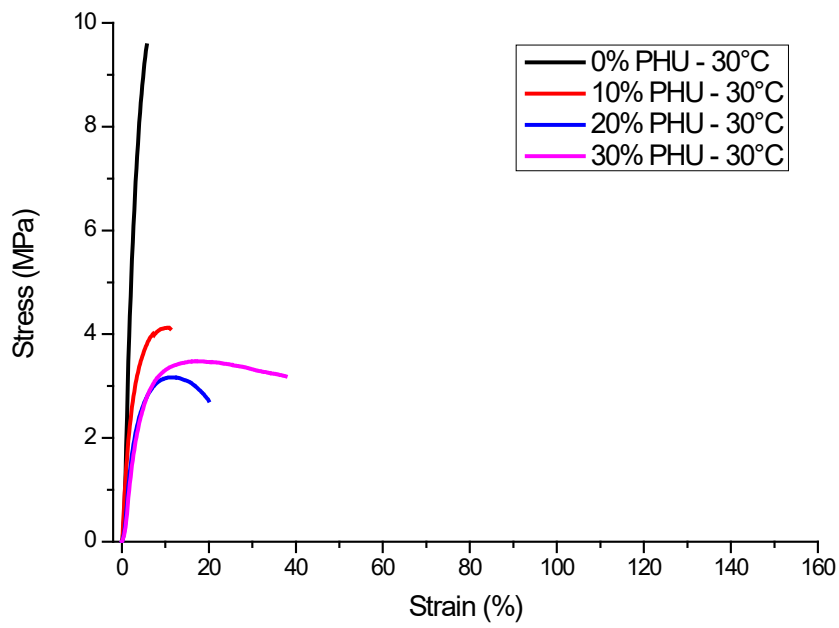


Figure 5. Effect of the of the PHU content and casting temperature on the stress-strain curves.

Table 3. Tensile test results of the cast films depending on the casting temperature as well as the PHU content

Temperature [°C]	PHU Content [%]	Young Modulus [MPa]	Strain at break [%]	Stress at break [MPa]	Toughness [MPa]
30	0	336 ± 49	5.7 ± 2.5	9.9 ± 3.7	0.32 ± 0.22
30	10	161 ± 13	6.7 ± 5.1	4.8 ± 1.7	0.22 ± 0.21
30	20	111 ± 11	20 ± 11.9	3.1 ± 0.8	0.54 ± 0.51
30	30	63 ± 21	38.6 ± 10.3	2.7 ± 0.7	0.95 ± 0.13
45	20	126 ± 18	132.1 ± 55.2	3.1 ± 0.5	4.53 ± 2.08
60	20	101 ± 6	38.4 ± 5.3	3.8 ± 0.4	1.3 ± 0.3

Figure 6 presents the TEM images of microtome cuts of the films cast from the 20 wt% PHU at different temperatures. The images showed some dark zones that were attributed to PHU aggregates because their size increased with the casting temperature and in soft-hard polymer-polymer hybrids, it is known that the softer polymer undergoes substantial migration forming large aggregates.^{31,35} In order to confirm that aggregates of PHU are formed, AFM measurements were carried out for the films containing 0 wt% and 30 wt% of PHU. The results presented in Figure 7 clearly show that the PHU migrated to form clusters. The TEM images for 30°C and 45°C were not that different, whereas that of the film cast at 60°C showed a clear phase separation. It can be then speculated that increasing the casting temperature allowed a better packing of the particles and perhaps some interpenetration of the polymer located in different particles. This is an effect similar to that of the coalescent agents. However, above a certain casting temperature, phase migration was possible leading to a strong phase separation and lower mechanical properties.

These tunable different results showed that by simply varying the PHU content and the casting conditions, coatings with tunable mechanical properties can be obtained. Combination of these characteristics with the versatility of the synthetic method opens

the possibility for obtaining a broad range of new environmentally friendly VOC-free waterborne urethane-(meth)acrylic coatings and adhesives.

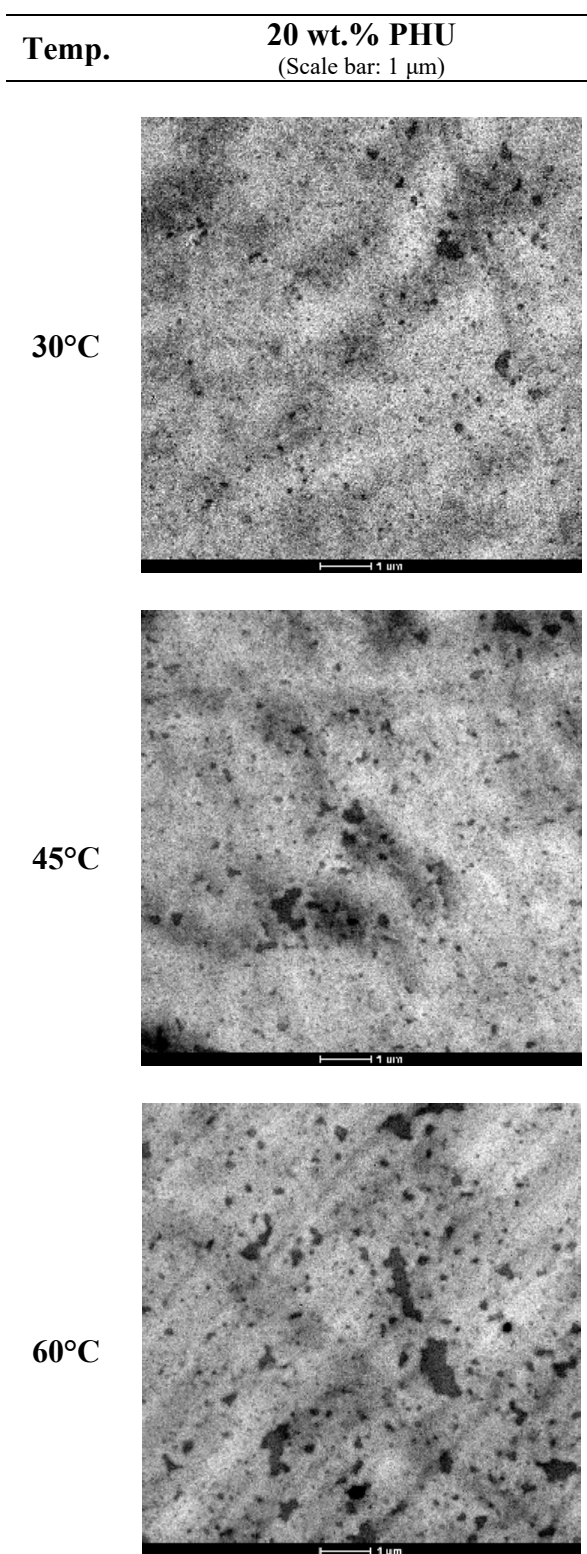
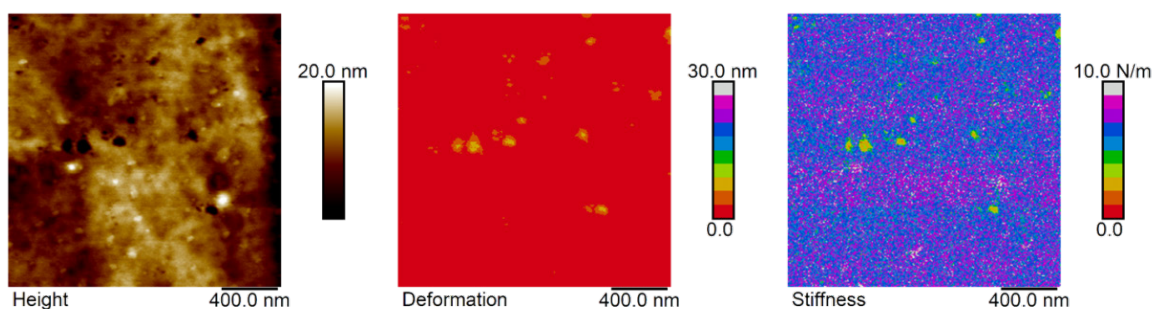


Figure 6. TEM pictures of cryo-microtome cuts of film prepared with the 20 wt% PHU hybrid at different temperatures. No staining was used.

a) 0 wt% PHU



b) 30 wt% PHU

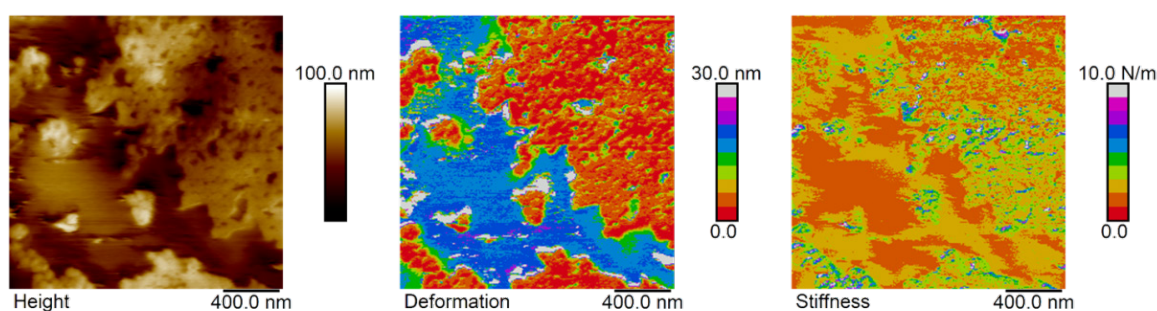


Figure 7. AFM pictures (peak force mode) of the films cast at 30°C from the latexes containing a) 0 wt.% PHU and b) 30 wt.% PHU

3. Conclusions

In this work, a VOC-free method for the synthesis of PHU-(meth)acrylic waterborne hybrid dispersions was developed. The PHU was first synthesized by bulk aminolysis of cyclic-carbonate derivatives using bio-sourced vegetable oil-based diamines. Then, the PHU was dissolved in (meth)acrylate monomers and the mixture used as the organic phase of a miniemulsion. Subsequent free radical polymerization of the (meth)acrylic monomers led to the hybrid PHU/(meth)acrylates waterborne dispersions. The choice of the initiator system was critical to achieve coagulum-free dispersions. Both AIBN and TBHP/ascorbic acid could be used, but the redox system offered advantages for scaling up. The synthetic method is very versatile and is not restricted in terms of the (meth)acrylate monomers.

Hybrid dispersions containing up to 30 wt.% of PHU were prepared obtaining particles with a core-shell morphology with the PHU in the shell. Transparent films were obtained for all compositions, but some yellowing appeared as the PHU content increased. The minimum film formation temperature (MFFT) decreased with the PHU content. Tensile tests showed that by simply varying the PHU content and the casting conditions, coatings with widely different mechanical properties can be obtained.

It is hoped that the availability of this environmentally friendly and versatile synthetic method (both in terms of monomers as well as film casting conditions) will foster the search of new environmentally friendly waterborne urethane-acrylic coatings and adhesives.

4. Experimental

4.1. Materials. 1,4-butanediamine (4DA, >98%), decane 1,10-diamine (10DA, >98%) and 1,12-diaminododecane (12DA, >98%) were supplied by TCI Europe. 1,6-hexanediamine (6DA, >99%) was obtained from Accros. 1,3-cyclohexanebis(methylamine) (CycloDA, 98%), butyl acetate (BAc, >99%), butyl acrylate (BA, >99%), butyl methacrylate (BMA, 99%), stearyl acrylate (SA, 97%), 2,2'-azobis(2-methylpropionitrile) (AIBN, 98%), benzoyl peroxide (BPO, 75%) and tert-butyl hydroperoxide (TBHP, 70% in water) were obtained from Sigma. Sebacoyl Chloride (97%) was obtained from Alfa Aesar. Glycerol 1,2-carbonate (90%) was purchased at ABCR. Ascorbic acid (or Vitamin C, AsA, >99.5%) was obtained from Fluka. Trimethylamine (NEt₃, 99%) was provided by Fisher. Dichloromethane (DCM) was obtained from VWR Chemicals. Croda kindly provided Priamine™ 1075 (P1075). Dow kindly provided alkyl diphenyl oxide disulfonate (Dowfax™ 2A1, D2A1, 45wt% in water). Deionized water was used.

4.2. Synthesis of the bis-cyclic carbonate (bisCC-C₁₀). The bis-cyclic carbonate monomer (bisCC-C₁₀) was synthesized according to the following strategy. In a three-neck round bottom flask, 2.2 eq. (30 g, 254 mmol) of glycerol carbonate and 2.2 eq. (25.707 g, 254 mmol) of trimethylamine were added to 100 mL of dichloromethane (DCM). This mixture was cooled down with the help of an ice bath and 1 eq. (27.615 g, 115.5 mol) of sebacoyl chloride was added dropwise. The reaction mixture was left under stirring for 24 h at room temperature. After reaction, the product was purified by means of the following liquid-liquid extraction steps: 5 times with 200 mL of an acid solution (5wt.% HCl), followed by 3 times with a basic treatment (stirring with basic alumina during 1h, followed by filtration of the liquid DCM phase) and finally 1 washing step with brine. The isolated organic phase was then dried with MgSO₄, filtered over a sintered filter and the dichloromethane was removed under reduced pressure. The obtained white powder was then analyzed by ¹H-NMR. The white powder was dried in a vacuum oven at 40°C overnight to remove any traces of remaining solvent. Yield: 50 %

¹H-NMR: δ H (400 MHz, DMSO-d₆) 5.10 – 4.97 (2 H, m), 4.57 (2 H, t), 4.43 – 4.17 (6 H, m), 2.33 (4 H, t), 1.51 (4 H, q), 1.25 (8 H, d).

The reaction scheme and the NMR spectra are provided in the Supporting Information (Figure S1).

4.3. PHU synthesis. As explained in the introduction, two synthetic strategies were explored. The first strategy involves the aminolysis of cyclic carbonates with diamines in (meth)acrylic monomers, followed by dispersion in water and subsequent free radical polymerization of the (meth)acrylates.

Regarding the first strategy, in a three-neck round bottom flask, a 10 wt.% of a stoichiometric mixture of bisCC-C₁₀ and P1075 were dissolved in butyl acrylate (BA) or

butyl methacrylate (BMA) and the solution was kept at 70°C for 16h. The reaction temperature was then increased up to 90°C during 9h. The same reaction was performed in butyl acetate (BAc) as a reference reaction to highlight the effect of the vinyl moiety of BA. The reaction was monitored by means of ¹H-NMR analyses in CDCl₃.

In the second strategy, poly(hydroxy)urethanes (PHUs) were synthesized through the aminolysis reaction between bisCC-C₁₀ and P1075 (Scheme 1). The stoichiometric ratio for the reactive moieties was used to target high molar masses according to Carother's theory.²⁶ The reactions were performed in bulk at 90°C for 24h in a Schlenk tube using a helical shaped mechanical stirrer specifically designed to fit in the Schlenk vessel. No catalyst was added for the polymerization reactions. No purification of the PHUs was performed after reaction.

4.4. PHU solubility. The solubility of bisCC-C₁₀, a series of diamines and the resulting PHUs in BMA was determined. The diamines used were 1,4-butanediamine (4DA), 1,6-hexanediamine (6DA), 1,10-diaminodecane (10DA), 1,12-diaminododecane (12DA), 1,3-cyclohexanebis(methylamine) (CycloDA), PriamineTM 1075 (P1075) (Scheme S3). The monomers were added so that the total concentration of monomers reached 10 wt.% of the resulting mixture. The reaction was then left to proceed at 80°C during 24h under magnetic stirring. The influence of the targeted polymer chain length was also investigated by varying the cyclic carbonate/diamine ratio according to Carother's theory (details in SI).

4.5. Miniemulsification and miniemulsion polymerization. The formulations used are summarized in Supporting Information (Tables S4 and S5). The organic phase of the miniemulsion was prepared by dissolving P1075-based PHU (0 to 30 wt% based on BMA) in a mixture of BMA and SA (4 wt% of SA) at 80°C. The aqueous phase was a 1 wt% (based on the total organic phase) solution of Dowfax 2A1 in deionized water. The

organic phase was added drop-wise into the aqueous phase under vigorous magnetic stirring. Then, the miniemulsion was formed by sonicating the coarse emulsion for 30 min with a Hielscher Ultrasonics GmbH (ref UIS250V) using an amplitude of 100% and 0.8s duty cycle. A post-stabilization step is performed by adding 1 wt% of Dowfax 2A1 based on the total organic phase dissolved in a minimum amount of deionized water.

The miniemulsion was transferred to a 3-neck round-bottom flask and flushed with nitrogen during 30 min at 70°C. The TBHP was added to the miniemulsion as soon as it was placed in the 3-neck round-bottom flask, giving time to TBHP to partition between the aqueous and organic phases during the nitrogen purging. When the nitrogen flushing was over, an aqueous solution of AsAc was fed in a semicontinuous mode during 2 to 3 h depending on the reaction.

The reaction mixture was left under magnetic stirring at 70°C for a reaction time ranging from 1h30 to 5h30. Regular sampling was performed in order to monitor the conversion (by gravimetry) and the particle size (by dynamic light scattering, DLS). At the end of the reaction, the latex was cooled down to room temperature and filtered through an 85 μm *Nylon* mesh in order to collect the fraction of polymer coagulated.

4.6. Film casting. The films were obtained by casting the latexes in silicon molds at 30 °C and 55% relative humidity for 48 hours. Rectangular specimens were cast for tensile tests (10 x 40 x 0.3 mm³). Square samples were cast for TEM and AFM analyses (10 x 10 x 0.5 mm³). These square samples were cut with a cryo-microtome device. In order to study the effect of the casting temperature on film morphology, some films were also cast at 45°C and 60°C (55% relative humidity, 24 hours).

4.7. Characterization. Monomer conversion was determined by gravimetry, which measures the conversion of volatile monomers. SA is not volatile as it has a boiling point of about 400 °C. Therefore, gravimetric conversions refer to BMA.

¹H-NMR spectra were recorded on a Bruker Avance 400 spectrometer (400.20 MHz or 400.33 MHz) by using DMSO-d₆ or CDCl₃ as a solvent at room temperature.

The coagulum fraction was measured by filtration of the latex through an 85 μm nylon mesh.

Monomer droplet sizes as well as particle sizes were measured by dynamic light scattering in a Zetasizer Nano Z (Malvern Instruments). The samples were prepared by dilution of the latex in deionized water. The equipment was operated at 25 °C and the values reported are the z-average values. They are the average of three repeated measurements after 15 sec equilibration time at the programmed temperature.

The molar masses of the soluble fraction of the polymer latexes were determined by SEC/MALLS/RI. The equipment was composed of a LC20 pump (Shimadzu) coupled to a DAWN Heleos II multiangle (18 angles) light scattering laser photometer equipped with an He-Ne laser ($\lambda = 658$ nm), and Optilab Rex differential refractometer ($\lambda = 658$ nm), all from Wyatt Technology Corp., USA. Separation was carried out using three columns in series (Styragel HR2, HR4, and HR6; with pore sizes from 10² to 10⁶ Å). The analyses were performed at 35°C and THF was used as mobile phase at a flow rate of 1 mL.min⁻¹.

The molar masses of the PHUs were also determined by Size Exclusion Chromatography (SEC) using dimethylformamide (DMF + lithium bromide LiBr 1g/L) as the eluent. Measurements in DMF were performed on an Ultimate 3000 system from Thermoscientific equipped with diode array detector. The system also includes a differential refractive index detector (dRI) from Wyatt technology. Polymers were

separated on two KD803 Shodex gel columns and one KD804 Shodex gel columns (300 x 8 mm) (exclusion limits from 1000 Da to 700 000 Da) at a flow rate of 0.8 mL/min. Column temperature was held at 50°C. Easivial kit of Polystyrene from Agilent was used as the standard (Mn from 162 to 364 000 Da).

Particle and film morphologies were analyzed by transmission electron microscopy (TEM) in a TECNAI G² 20 TWIN microscope operated at 200 kV and equipped with LaB6 filament, and high angle annular dark-field-scanning transmission electron microscopy (HAADF-STEM). When analyzing the particle morphologies, the samples were previously stained with phosphotungstic acid (PTA) by adding 2 wt% of PTA to the diluted latex. The mixture of diluted latex and PTA was sonicated for 30 min at maximum power in a Bandelin Sonorex sonicator. A drop of this solution was spin-coated onto a carbon-coated copper grid (300mesh) at 1500 rpm for 3 min. In order to analyze the film morphologies, ultra-thin sections of about 80 nm of thickness were obtained at -25°C temperature using a cryo-ultramicrotome device (Leica UC6FC6) equipped with a diamond knife. The ultrathin sections were placed on 300 mesh copper grids. They were analyzed without any staining.

Film morphologies were also analyzed by means of atomic force microscopy (AFM). The films were cut with a cryo-microtome device equipped with a diamond knife (described in the TEM section). The AFM data were directly acquired onto the surface area of the cut film, which was left tight in a specially designed sample holder that was used for cutting the film in the microtome. The peak force quantitative nanomechanical mapping (PF-QNM) method was used for characterization purposes, which allows for the simultaneous recording of topography as well as mechanical properties. The AFM images were acquired at 25°C and 55% relative humidity, using a Multimode 8 microscope and a Nanoscope V controller (Bruker). All the images were processed offline

using the commercial software Nanoscope Analysis 1.9 (Bruker). Considering that the images were acquired from the surface area of the films that were still located in the microtome's holder, all the samples were thick enough to avoid any effect of the supporting substrate in the measurement of the nanomechanical properties. The basic idea of the PF-QNM technique, extensively described in the work of Limousin *et al.*³¹ and references therein, consists in recording dynamic force curves in a pixel-wise fashion. These curves represent the applied force on the probe while it approaches and retracts from the film surface, as a function of the tip-sample distance and/or interaction time. The user defined feedback parameter, called 'peak force', relates to the maximum load applied to the surface. In the present work, a value of 10 nN was used. We obtained PF-QNM maps with a 256 x 256 resolution, and a frequency modulation (f_m) of 2 kHz. In PF-QNM, the analysis of the force-distance curves allows the calculation of different nanomechanical maps. In this work, we present the deformation and stiffness maps of the investigated samples. The deformation is a parameter related to the distance penetrated by the AFM tip into the film surface. The stiffness relates to the resistance opposed by the sample to the tip penetration. This latter parameter was calculated as the slope of the approached part of the force-curve distance, by a linear fit. To obtain PF-QNM quantitative maps, the relative calibration method proposed by Bruker and recently used in the literature was followed.^{31,36,37} All samples were probed using Tap 150AI-G probes, by BudgetSensors (tip radius <10 nm, as estimated from a tip-checker sample provided by Bruker). The deflection sensitivity of the detector was obtained using a sapphire sample, provided by Bruker. Finally, the spring constant was determined to be ~ 3 N/m according to the Sader method.³⁸

Differential Scanning Calorimetry (DSC) thermograms were measured using a DSC Q100 apparatus from TA Instruments using a heating ramp at $10^\circ\text{C}\cdot\text{min}^{-1}$ from -80°C to

130°C. The first heating ramp was used to measure the glass transition temperatures (T_{gs}) in order to get a picture of the properties of the cast films.

The minimum film formation temperature (MFFT) was determined on a steel bar with a temperature gradient that was measured with thermocouples located at regular distances. A thin layer of latex was applied onto the MFFT bar with a film applicator (60 μm thickness) and the water was left to evaporate so that the film can form. The MFFT was defined as the temperature at which both a clear coat was observed and a clear cut could be made with a knife without forming any powder.

Tensile stress-strain measurements were carried out from the cast rectangular films with a texture analyzer (Stable Micro Systems Ltd., Godalming, UK) at a constant velocity of 0.42 $\text{mm}\cdot\text{s}^{-1}$. The size of the samples was 10 x 40 x 0.3 mm^3 . The reported results were the average of at least 3 repeated tensile tests of 3 different specimens. The Young's modulus was determined as the slope of the stress-strain curve at low strain (in the elastic region – before the yield point) and the toughness was calculated as the area under the obtained curve.

ASSOCIATED CONTENT

Supporting Information. Characterization of bisCC-C₁₀, the studied on side-reactions and monomer solubilities, the results with thermal initiators, the formulations with redox initiators, SEC-MALLS traces, DSC traces and the measurements of the MFFTs can be found in the Supporting Information. Figures S1 to S13, Tables S1 to S6, Schemes S1 to S3 (PDF).

AUTHOR INFORMATION

Corresponding Authors

* Henri Cramail - cramail@enscbp.fr

* José M. Asua – jm.asua@ehu.eus

Author Contributions

The manuscript was written through contributions of all authors. All authors have given approval to the final version of the manuscript.

Notes

The authors declare no competing financial interest.

ACKNOWLEDGMENT

BB acknowledges both the University of Bordeaux (UB) as well as POLYMAT for funding. From the UB side, this project has benefited from state funding, managed by the French National Research Agency (ANR). The funding is allocated in the framework of the “Investments for the Future” program, with the reference number ANR - n ° ANR-10-IDEX-03-02.

REFERENCES

- (1) Adam, N.; Avar, G.; Blankenheim, H.; Friederichs, W.; Giersig, M.; Weigand, E.; Halfmann, M.; Wittbecker, F.-W.; Larimer, D.-R.; Maier, U.; et al. Polyurethanes. In *Ullmann's Encyclopedia of Industrial Chemistry*; Wiley-VCH Verlag GmbH & Co. KGaA., Ed.; Major Reference Works; 2005.
- (2) Yilgör, I.; Yilgör, E.; Wilkes, G. L. Critical Parameters in Designing Segmented Polyurethanes and Their Effect on Morphology and Properties: A Comprehensive Review. *Polymer (Guildf)*. **2015**, *58*, A1–A36.
- (3) Król, P. Synthesis Methods, Chemical Structures and Phase Structures of Linear

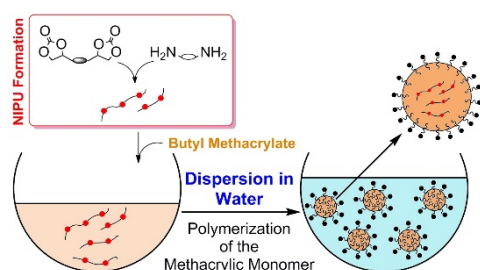
- Polyurethanes. Properties and Applications of Linear Polyurethanes in Polyurethane Elastomers, Copolymers and Ionomers. *Progress in Materials Science*. August 2007, pp 915–1015.
- (4) Kim, B. K.; Lee, J. C. Modification of Waterborne Polyurethanes by Acrylate Incorporations. *J. Appl. Polym. Sci.* **1995**, *58* (7), 1117–1124.
 - (5) Okamoto, Y.; Hasegawa, Y.; Yoshino, F. Urethane/ Acrylic Composite Polymer Emulsions. *Prog. Org. Coatings* **1996**, *29*, 175–182.
 - (6) Manock, H. L. New Developments in Polyurethane and PU/Acrylic Dispersions. *Pigment Resin Technol.* **2000**, *29* (3), 143–151.
 - (7) Mehravar, S.; Ballard, N.; Tomovska, R.; Asua, J. M. Polyurethane/Acrylic Hybrid Waterborne Dispersions: Synthesis, Properties and Applications. *Ind. Eng. Chem. Res.* **2019**, *58*, 20902–20922.
 - (8) Karol, M. H.; Kramarik, J. A. Phenyl Isocyanate Is a Potent Chemical Sensitizer. *Toxicol. Lett.* **1996**, *89* (2), 139–146.
 - (9) Pollaris, L.; Devos, F.; De Vooght, V.; Seys, S.; Nemery, B.; Hoet, P. H. M.; Vanoirbeek, J. A. J. Toluene Diisocyanate and Methylene Diphenyl Diisocyanate: Asthmatic Response and Cross-Reactivity in a Mouse Model. *Arch. Toxicol.* **2016**, *90* (7), 1709–1717.
 - (10) Bolognesi, C.; Baur, X.; Marczynski, B.; Norppa, H.; Sepai, O.; Sabbioni, G. Carcinogenic Risk of Toluene Diisocyanate and 4,4'-Methylenediphenyl Diisocyanate: Epidemiological and Experimental Evidence. *Crit. Rev. Toxicol.* **2001**, *31* (6), 737–772.
 - (11) Wang, C.; Chu, F.; Graillat, C.; Guyot, A.; Gauthier, C.; Chapel, J. P. Hybrid Polymer Latexes: Acrylics-Polyurethane from Miniemulsion Polymerization: Properties of Hybrid Latexes versus Blends. In *Polymer*; Elsevier BV, 2005; Vol. 46, pp 1113–1124.
 - (12) Wang, C.; Chu, F.; Graillat, C.; Guyot, A.; Gauthier, C. Hybrid Polymer Latexes - Acrylics-Polyurethane: II. Mechanical Properties. *Polym. Adv. Technol.* **2005**, *16* (2–3), 139–145.
 - (13) Li, M.; Daniels, E. S.; Dimonie, V.; David Sudol, E.; El-Aasser, M. S. Preparation of Polyurethane/Acrylic Hybrid Nanoparticles via a Miniemulsion Polymerization Process. *Macromolecules* **2005**, *38* (10), 4183–4192.
 - (14) Mehravar, S.; Ballard, N.; Agirre, A.; Tomovska, R.; Asua, J. M. Relating Polymer Microstructure to Adhesive Performance in Blends of Hybrid Polyurethane/Acrylic Latexes. *Eur. Polym. J.* **2017**, *87*, 300–307.
 - (15) Mehravar, S.; Ballard, N.; Agirre, A.; Tomovska, R.; Asua, J. M. Role of Grafting on Particle and Film Morphology and Film Properties of Zero VOC Polyurethane/Poly(Meth)Acrylate Hybrid Dispersions. *Macromol. Mater. Eng.* **2019**, *304* (2), 1800532.
 - (16) Mehravar, S.; Roschmann, K. J.; Arocha, P. U.; Reck, B.; Agirre, A.; Tomovska, R.; Asua, J. M.; Ballard, N. Correlating Microstructure and Performance of

- PU/(Meth)Acrylic Hybrids as Hardwood Floor Coating. *Prog. Org. Coatings* **2019**, *131*, 417–426.
- (17) Mehravar, S.; Ballard, N.; Tomovska, R.; Asua, J. M. The Influence of Macromolecular Structure and Composition on Mechanical Properties of Films Cast from Solvent-Free Polyurethane/Acrylic Hybrid Dispersions. *Macromol. Mater. Eng.* **2019**, *304* (8), 1900155.
- (18) Mehravar, S.; Ballard, N.; Veloso, A.; Tomovska, R.; Asua, J. M. Toward a Green Synthesis of Polyurethane/(Meth)Acrylic Dispersions through Control of Colloidal Characteristics. *Langmuir* **2018**, *34* (39), 11772–11783.
- (19) Meng, L.; Wang, X.; Ocepek, M.; Soucek, M. D. A New Class of Non-Isocyanate Urethane Methacrylates for the Urethane Latexes. *Polymer (Guildf)*. **2017**, *109*, 146–159.
- (20) Meng, L.; Soucek, M. D.; Li, Z.; Miyoshi, T. Investigation of a Non-Isocyanate Urethane Functional Monomer in Latexes by Emulsion Polymerization. *Polymer (Guildf)*. **2017**, *119*, 83–97.
- (21) Maisonneuve, L.; Lamarzelle, O.; Rix, E.; Grau, E.; Cramail, H. Isocyanate-Free Routes to Polyurethanes and Poly(Hydroxy Urethane)S. *Chem. Rev.* **2015**, *115*, 12407–12439.
- (22) Cornille, A.; Auvergne, R.; Figovsky, O.; Boutevin, B.; Caillol, S. A Perspective Approach to Sustainable Routes for Non-Isocyanate Polyurethanes. *Eur. Polym. J.* **2017**, *87*, 535–552.
- (23) Carré, C.; Ecochard, Y.; Caillol, S.; Avérous, L. From the Synthesis of Biobased Cyclic Carbonate to Polyhydroxyurethanes: A Promising Route towards Renewable Non-Isocyanate Polyurethanes. *ChemSusChem* **2019**, *12* (15), 3410–3430.
- (24) Asua, J. M. Miniemulsion Polymerization. *Prog. Polym. Sci.* **2002**, *27*, 1283–1346.
- (25) Asua, J. M. Challenges for Industrialization of Miniemulsion Polymerization. *Prog. Polym. Sci.* **2014**, *39*, 1797–1826.
- (26) Odian, G. Step Polymerization. In *Principles of Polymerization*; John Wiley & Sons, Inc., 2004; pp 39–197.
- (27) Asua, J. M. Ostwald Ripening of Reactive Costabilizers in Miniemulsion Polymerization. *Eur. Polym. J.* **2018**, *106*, 30–41.
- (28) Taylor, M. A. Synthesis of Polymer Dispersions. In *Polymer Dispersions and Their Industrial Applications*; Wiley-VCH Verlag GmbH & Co. KGaA, 2003; pp 15–40.
- (29) Manea, M.; Chemtob, A.; Paulis, M.; de la Cal, J. C.; Barandiaran, M. J.; Asua, J. M. Miniemulsification in High-Pressure Homogenizers. *AIChE J.* **2008**, *54* (1), 289–297.
- (30) do Amaral, M.; Arevalillo, A.; Santos, J. L.; Asua, J. M. Novel Insight into the Miniemulsification Process: CFD Applied to Ultrasonication. *Prog. Colloid*

Polym. Sci. **2004**, *124*, 103–106.

- (31) Limousin, E.; Martinez-Tong, D. E.; Ballard, N.; Asua, J. M. Cure-Dependent Morphology of Acrylic/Alkyd Hybrid Latex Films via Nanomechanical Mapping. *ACS Appl. Polym. Mater.* **2019**, *1* (8), 2213–2223.
- (32) Limousin, E.; Ballard, N.; Asua, J. M. Synthesis of Cellulose Nanocrystal Armored Latex Particles for Mechanically Strong Nanocomposite Films. *Polym. Chem.* **2019**, *10* (14), 1823–1831.
- (33) Limousin, E.; Ballard, N.; Asua, J. M. The Influence of Particle Morphology on the Structure and Mechanical Properties of Films Cast from Hybrid Latexes. *Prog. Org. Coatings* **2019**, *129*, 69–76.
- (34) Limousin, E.; Ballard, N.; Asua, J. M. Soft Core-Hard Shell Latex Particles for Mechanically Strong VOC-Free Polymer Films. *J. Appl. Polym. Sci.* **2019**, *136* (23), 47608.
- (35) Goikoetxea, M.; Reyes, Y.; de las Heras Alarcón, C. M.; Minari, R. J.; Beristain, I.; Paulis, M.; Barandiaran, M. J.; Keddie, J. L.; Asua, J. M. Transformation of Waterborne Hybrid Polymer Particles into Films: Morphology Development and Modeling. *Polymer (Guildf)*. **2012**, *53* (5), 1098–1108.
- (36) Gojzewski, H.; Imre, B.; Check, C.; Chartoff, R.; Vancso, J. Mechanical Mapping and Morphology across the Length Scales Unveil Structure-Property Relationships in Polycaprolactone Based Polyurethanes. *J. Polym. Sci. Part B Polym. Phys.* **2016**, *54* (22), 2298–2310.
- (37) Gojzewski, H.; Obszarska, J.; Harlay, A.; Hempenius, M. A.; Vancso, G. J. Designer Poly(Urea-Siloxane) Microspheres with Controlled Modulus and Size: Synthesis, Morphology, and Nanoscale Stiffness by AFM. *Polymer (Guildf)*. **2018**, *150*, 289–300.
- (38) Sader, J. E.; Chon, J. W. M.; Mulvaney, P. Calibration of Rectangular Atomic Force Microscope Cantilevers. *Rev. Sci. Instrum.* **1999**, *70* (10), 3967–3969.

TABLE OF CONTENT



For table of content use only

Supporting Information

VOC-free Synthesis of Waterborne Poly(hydroxy urethane)- (meth)Acrylics Hybrids by Miniemulsion Polymerization

*Boris Bizet,^{ab} Etienne Grau,^a Henri Cramail^{*a} and José M. Asua^{*b}*

^a University of Bordeaux, CNRS, Bordeaux INP – LCPO, UMR 5629 – 16, Avenue Pey Berland, F-33600 Pessac, France

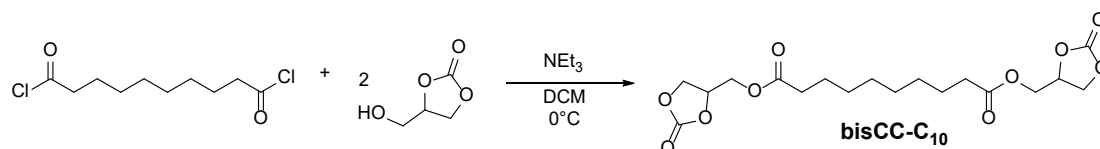
^b POLYMAT, University of the Basque Country UPV/EHU, Joxe Mari Korta Center, Avenida Tolosa 72, 20018 Donostia-San Sebastián, Spain

* Henri Cramail - cramail@enscbp.fr // * José M. Asua – jm.asua@ehu.eus

1. Reaction scheme and characterization of the sebacic acid-derived bis cyclic carbonate (bisCC-C ₁₀).....	2
2. First strategy: solution polymerization in a (meth)acrylic solvent.....	2
2.1. Side Reactions.....	2
2.2. Solubility.....	9
3. Study on thermal initiation.....	14
3.1. Formulations.....	15
3.2. Results & Discussion.....	16
4. Second strategy: Bulk formation of the PHU prior to incorporation into a (meth)acrylic solvent.....	18
4.1. Formulations with redox initiators.....	19
4.2. SEC-MALLS Traces.....	20
4.3. DSC Traces.....	21
4.4. Minimum Film Forming Temperature (MFFT).....	22
5. References.....	22

1. Reaction scheme and characterization of the sebacic acid-derived bis cyclic carbonate (bisCC-C₁₀)

a.



b.

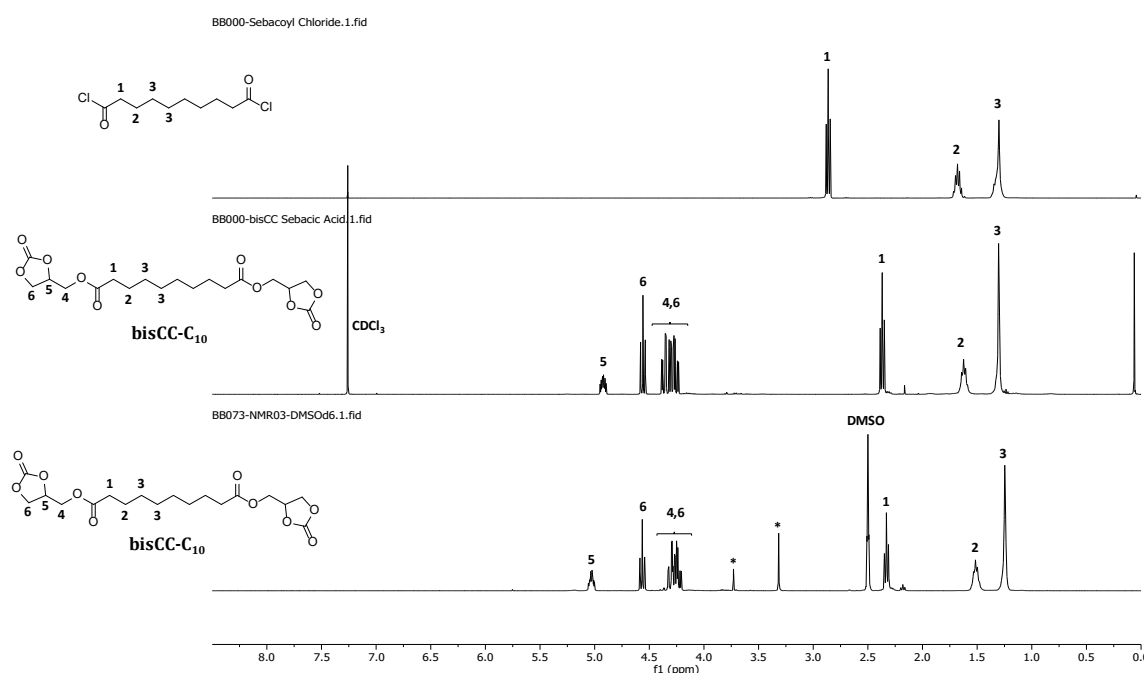


Figure S1: a) Synthetic route to bis cyclic carbonate (bisCC-C₁₀) from sebacoyl chloride and glycerol carbonate, and b) Stacked ¹H-NMR Spectra of Sebacoyl Chloride in CDCl₃ (top) and bisCC-C₁₀ in CDCl₃ (middle) and in DMSO-d₆ (bottom)

2. First strategy: solution polymerization in a (meth)acrylic solvent

2.1. Side Reactions

Amines and amine-terminated Non Isocyanate Polyurethanes (NIPUs) can potentially react with acrylic monomers, typically in an *aza*-Michael-type mechanism. During the aminolysis of cyclic carbonates to form poly(hydroxyurethane)s (PHU) carried out in the presence of acrylates, this side reaction will alter the stoichiometry amine/carbonate

lowering the molar mass. In order to check the occurrence of this reaction, 10 wt.% of a stoichiometric mixture of bisCC-C₁₀ and Priamine® 1075 (P1075) were dissolved in butyl acrylate (BA) and the solution was kept at 70°C for 16h. The reaction temperature was then increased up to 90°C during 9h. The same reaction was performed in butyl acetate (BAC) as a reference reaction to highlight the effect of the vinyl moiety of BA. The reaction was monitored by means of ¹H-NMR analyses in CDCl₃ and the results are given in Figure S2 to S5.

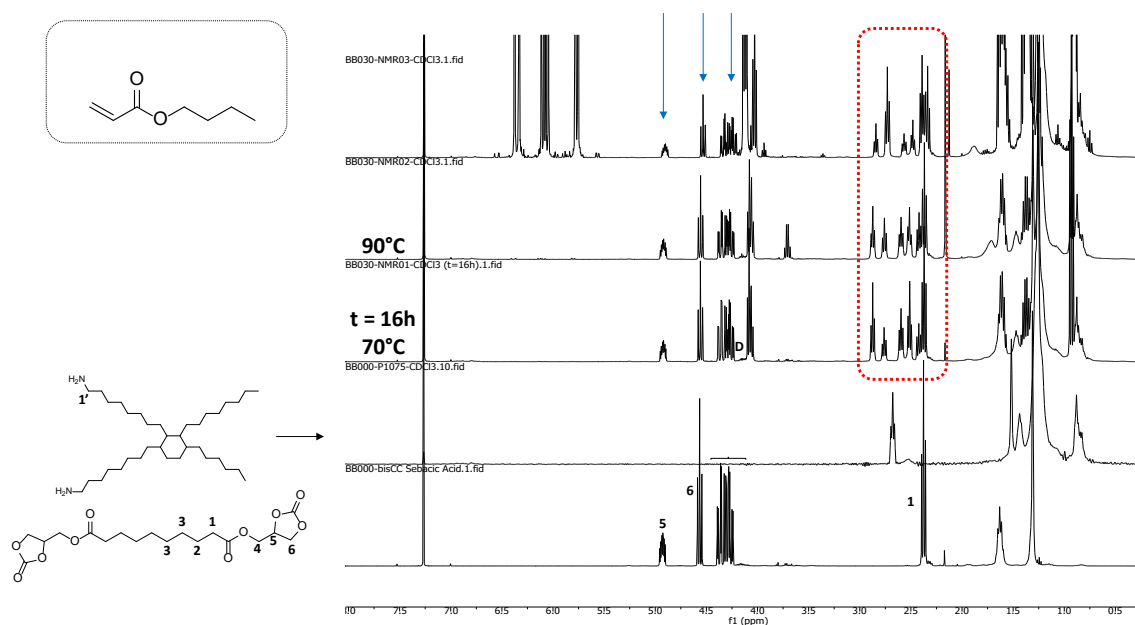


Figure S2: ¹H-NMR follow-up of the reaction of a stoichiometric mixture of bisCC-C₁₀ and P1075 in BA (10 wt % of the PHU monomers in BA)

The formation of the urethane moiety is usually observed thanks to the shift of the peak corresponding to the CH₂ moiety in alpha-position of the amine (1' in Figure S2). When located in alpha-position of a urethane moiety, it should appear in the region 2.9 to 3.4 ppm.¹ This shows that no PHU was formed in the process under the conditions used. This outcome was surprising since the formation of PHUs originating from the reaction between diamine and ester-activated bis-cyclic carbonates is known to take place at

temperatures as low as 20°C in bulk,¹ or at 70°C in dimethylformamide.² It can however be noticed that several peaks appeared in the region 2.3 to 2.7 ppm, suggesting the formation of by-products by side-reactions. In order to clarify if these by-products were the result of a reaction between BA and P1075, a reference reaction was run by removing bisCC-C₁₀ from the reactive mixture and the results are presented in Figure S3, where one can observe the peaks of the by-products.

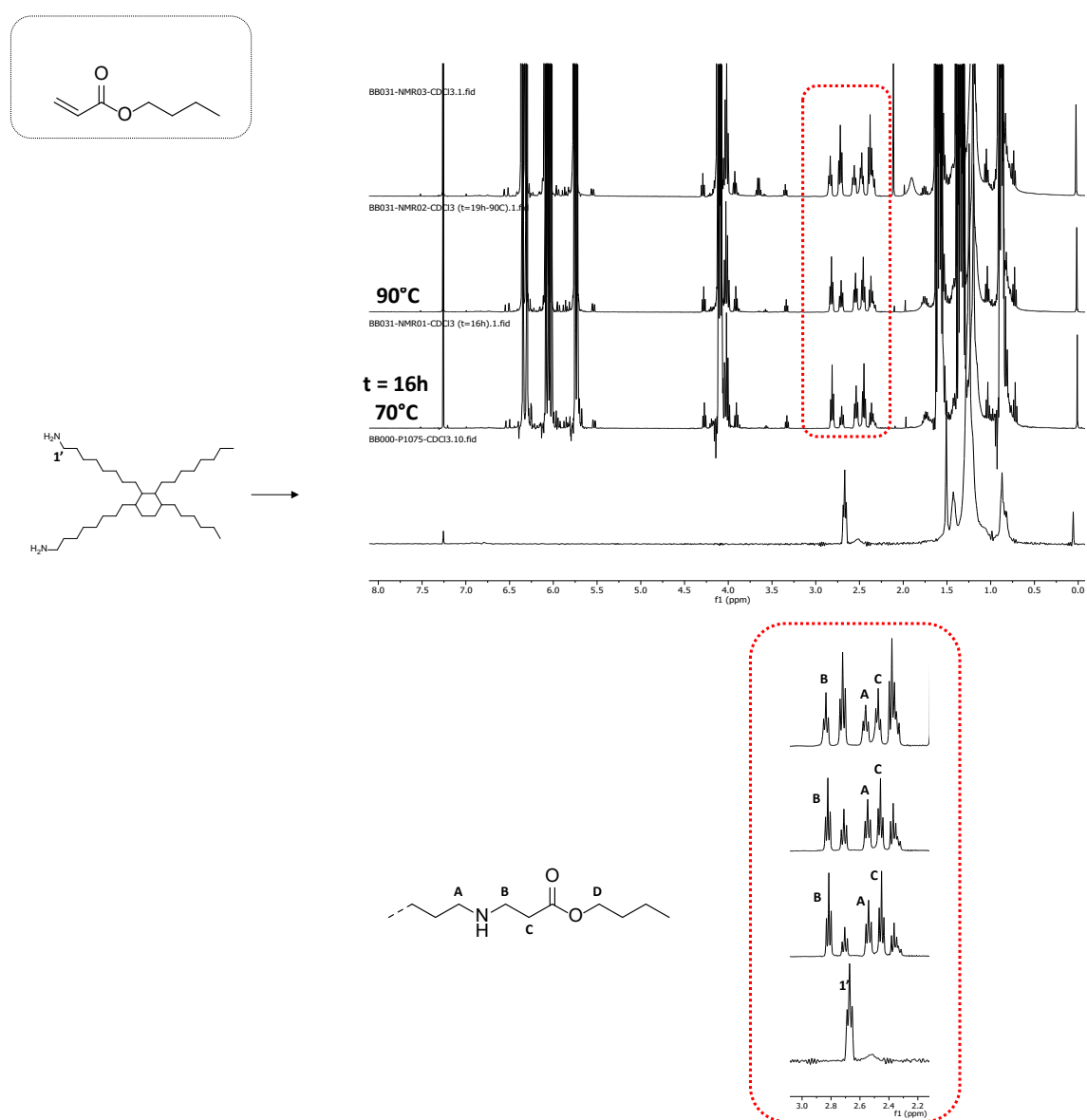
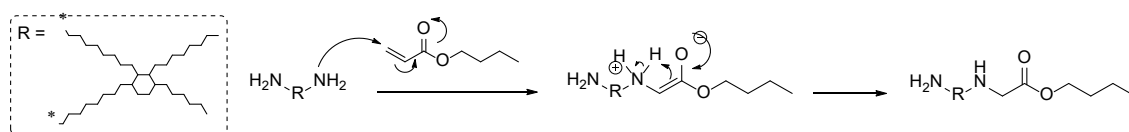


Figure S3: ¹H-NMR reaction follow-up (in CDCl₃) of P1075 in BA (same conditions as in Figure S2 without adding bisCC-C₁₀)

It was therefore clear that by-products were formed by reaction between P1075 and BA. Although all the products were not fully characterized and identified, the formation of adducts originating from an *aza*-Michael-type mechanism (Scheme S1) seems to account for the formation of some of the by-products and supports observations that have already been done in the literature.³⁻⁵ The NMR attribution was done according the work of Endo and coworkers.⁶



Scheme S1: Suggested mechanism for the *aza*-Michael addition of P1075 onto BA. Please note that for clarity purposes, only one amine moiety of the diamine was converted.

In order to check if the vinyl moiety was playing a role in the formation of the by-products, BA was replaced by butyl acetate (BAc). Similar to BA, two reactions were carried out: in the first one, a stoichiometric mixture of bisCC-C₁₀ and P1075 were reacted in BAc during 50h at 70°C. The second comparative reaction only used P1075 in BAc that were reacted at 70 °C during 19 h and then at 90 °C during 31 h. The resulting ¹H-NMR follow-ups in CDCl₃ are presented in Figure S4 and Figure S5 respectively.

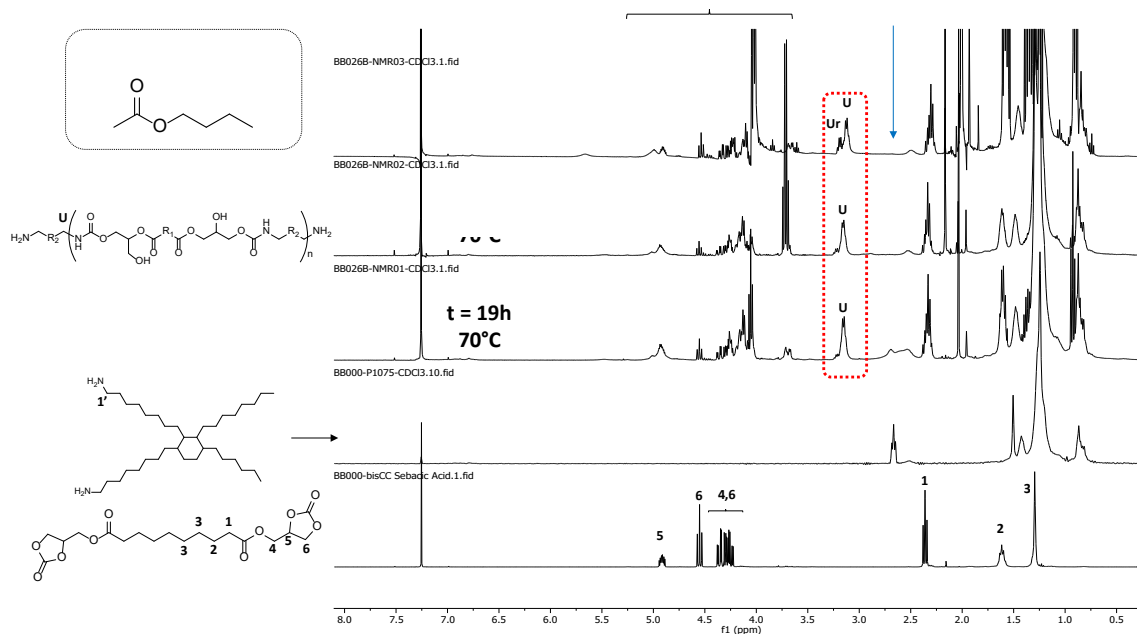
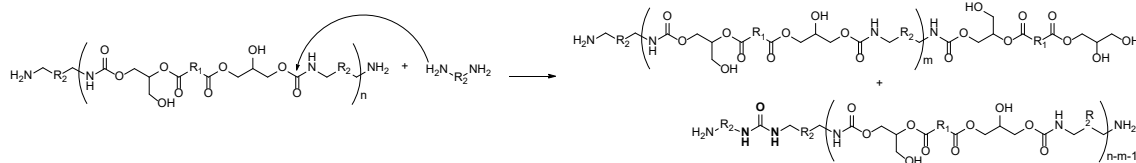


Figure S4: $^1\text{H-NMR}$ reaction follow-up (in CDCl_3) of the stoichiometric mixture of bisCC- C_{10} and P1075 in BAc.

The comparison between Figure S2 and Figure S4 shows that the PHU formation occurred in BAc as opposed to BA. This is attested by the shift of the peak corresponding to the protons attached to the carbon in α -position of the amine and/or urethane moieties from 2.7 to 3.2 ppm in the $^1\text{H-NMR}$ spectra. In addition, the formation of urea at long reaction times could be noticed after 27h of reaction and was clearly visible after 50h. This is the result of the reaction of amine moieties onto the already formed carbanate moieties, as described by Cramail and coworkers,² a reaction that is known to be hard to avoid.



Scheme S2: Urea formation by reaction of an amine moiety onto the PHU backbone.

Please note that for clarity purposes, only one amine moiety of the diamine was converted.

The reaction in BAc did not lead to the formation of the side-products that were observed in the case of BA, despite the longer reaction time. This may be due to the lack of vinylic moiety in BAc. In this way, the diamine remained available for the reaction with bisCC-C₁₀. To support this hypothesis, P1075 was dissolved in BAc without the presence of bisCC-C₁₀ and left at 70°C during 19h, and then at 90°C for 25h. The ¹H-NMR follow-up is presented in Figure S5 and clearly demonstrates that the amine did indeed not react with BAc.

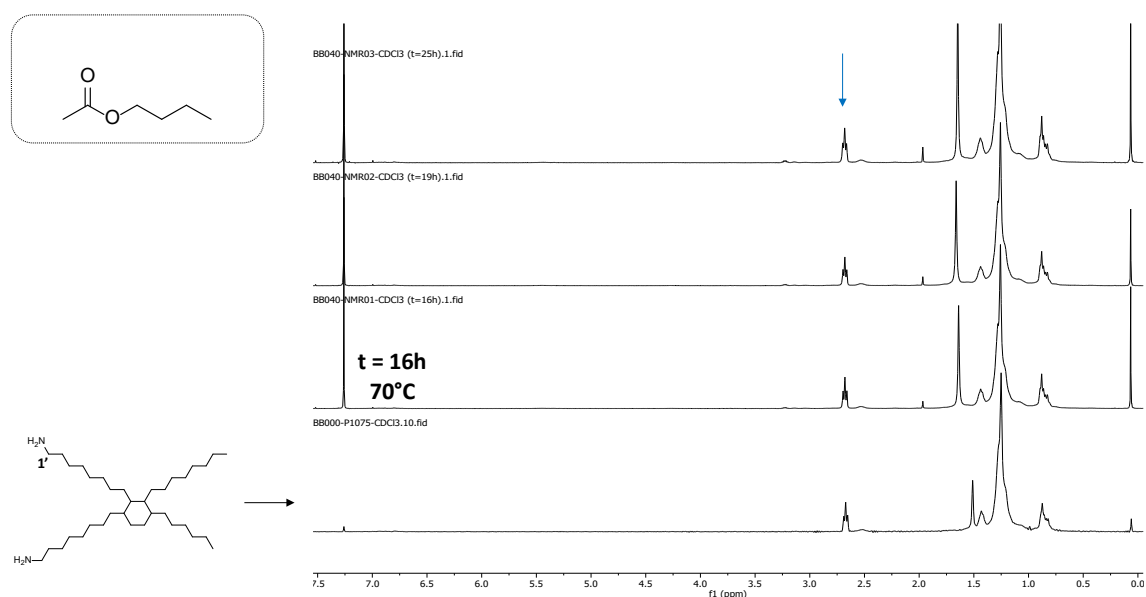


Figure S5: ¹H-NMR reaction follow-up (in CDCl₃) of P1075 in BAc

These results showed that acrylic monomers cannot be used as solvents for the synthesis of PHUs through aminolysis, because amines and acrylates undergo side-reactions. As methacrylates are in general less reactive than acrylates, it was decided to check if the side reactions could be avoided or at least minimized by using butyl methacrylate (BMA) instead of BA. The process was carried out under the same conditions than the ones utilized in the BA system (reaction at 70°C during 19h, and then further heating at 90°C during 23h). Figure S6 presents the variation of the ¹H-NMR spectra.

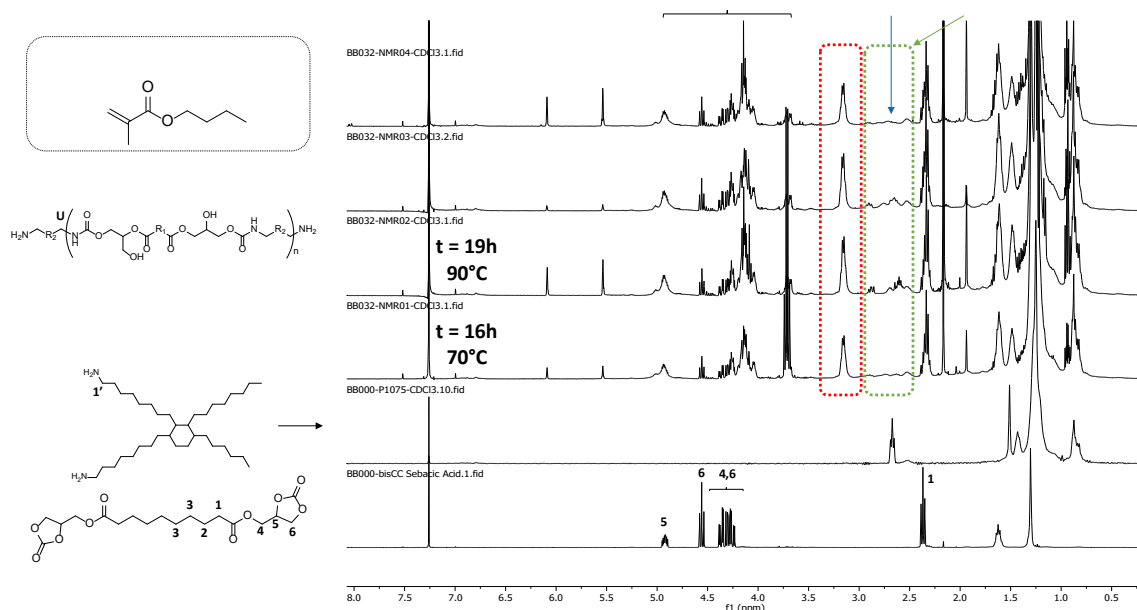


Figure S6: $^1\text{H-NMR}$ reaction follow-up (in CDCl_3) of the stoichiometric mixture of bisCC- C_{10} and P1075 in BMA

Figure S6 shows that the amine peak at 2.6 ppm disappeared and that the peak corresponding to the urethane at 3.2 ppm appeared, which are the fingerprints of the formation of PHU. The reaction kinetics was relatively fast (less than 24h) and side reactions were not significant. This suggests that the extent of side reactions (and in particular *aza*-Michael addition) is strongly diminished when methacrylates are used, which is in accordance with the results reported by Schimpf *et al.*⁵ The authors quantified the extent of the *aza*-Michael addition up to 10% (and 90% of hydroxyurethane) in the bulk reaction of stoichiometric amounts of glycerol carbonate methacrylate with primary amines at temperatures ranging from 60 to 100°C.

To further test these results, P1075 alone was put to react in BMA to see whether any trace of side reaction could be noticed (17h at 70°C followed by 22h at 90°C). The $^1\text{H-NMR}$ follow-up of the reaction is presented in Figure S7. It can be seen that almost no reaction was observed and the amine remained unreacted for 16h at 70°C followed by 9h

at 90°C (t=25h). After such a time, traces of new forming products could be identified in the NMR spectra around 2.5 and 2.8 ppm ranges. Nevertheless, as the formation of PHU occurs at shorter process times and lower reaction temperatures, methacrylates could be safely used as solvents in the formation of PHU by aminolysis reaction between diamines and cyclic carbonates.

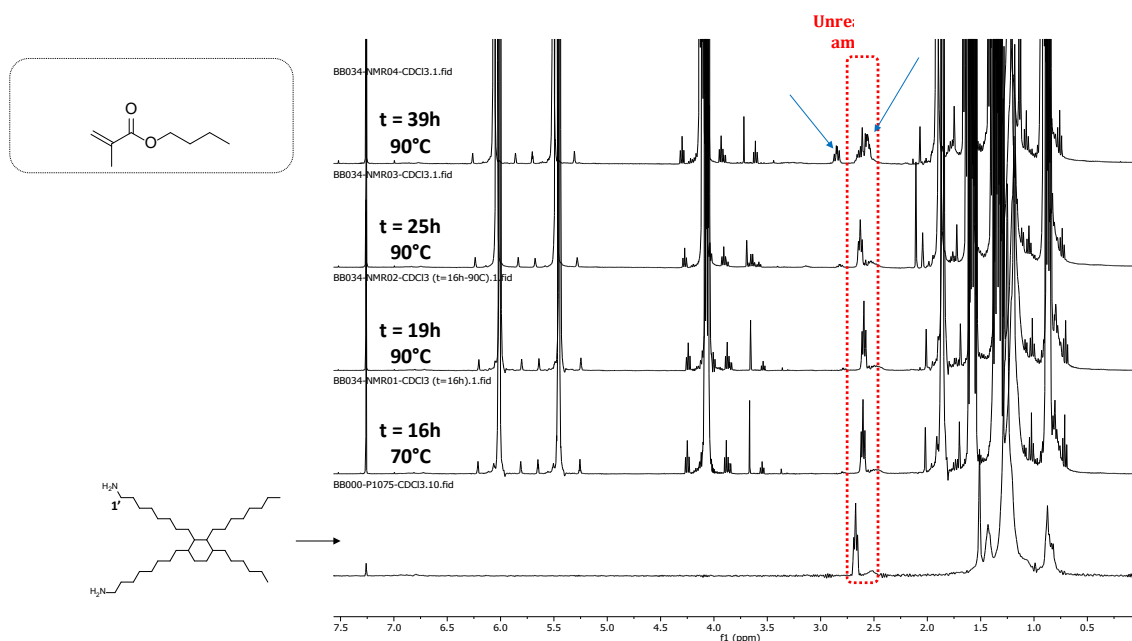


Figure S7: ^1H -NMR reaction follow-up (in CDCl_3) of P1075 in BMA.

2.2. Solubility

As the aminolysis reaction could be carried out in BMA without occurrence of side reactions, the solubility of bisCC-C₁₀, diamines and the resulting PHUs in BMA was determined. The diamines used were 1,4-butanediamine (4DA), 1,6-hexanediamine (6DA), 1,10-diaminodecane (10DA), 1,12-diaminododecane (12DA), 1,3-cyclohexanebis(methylamine) (CycloDA), PriamineTM 1075 (P1075) (Scheme S3).

The solubility of the monomers and that of the resulting PHU was determined. For this, the diamines were pre-heated in BMA during 30 min before the bisCC-C₁₀ was added.

The monomers were added so that the total concentration of monomers reached 10 wt.% of the resulting mixture. The reaction was then left to proceed at 80°C during 24h under magnetic stirring.

The influence of the targeted polymer chain length was also investigated by varying the cyclic carbonate/diamine ratio. Polymerizations involving stoichiometric amounts of monomers were also performed and will be labeled DP ∞ . According to Carother's theory,⁷ deviations from the stoichiometric ratio reduces the degree of polymerization (DP) of the resulting PHU chain. An excess of diamine was used in order to target DPs of 2 and 5. According to Carother's theory, the degree of polymerization, DP, is given by

$$DP = \frac{1 + r}{1 + r - 2rp} \quad (1)$$

where p is the conversion and r is the stoichiometric ratio between A-A and B-B reactants

$$r = \frac{n_{\text{CyclicCarbonate}}}{n_{\text{NH}_2}} \quad (2)$$

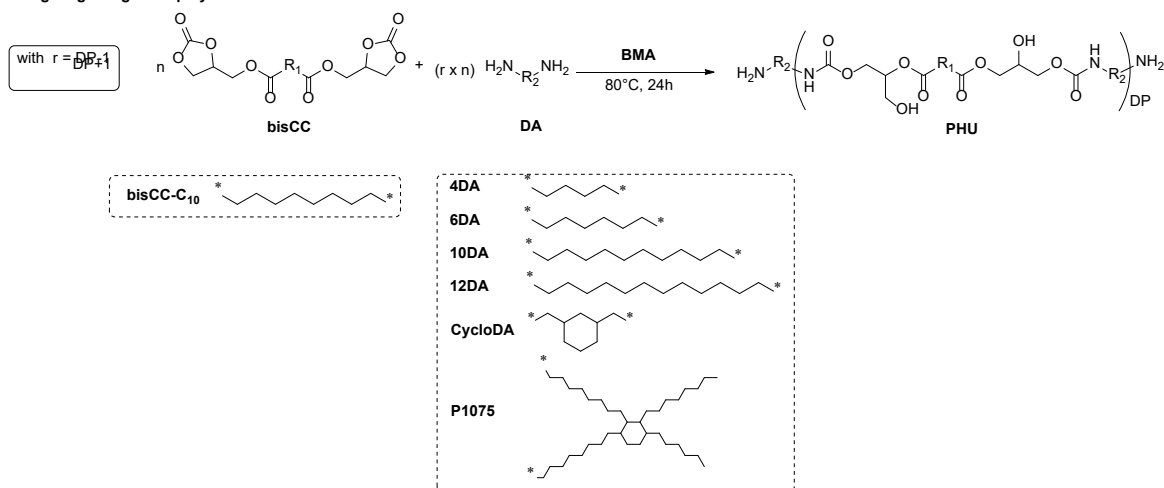
At complete conversion (p = 1), eq. 1 reduces to

$$DP = \frac{1 + r}{1 - r} \quad (3)$$

Which allows the calculation of the excess of diamine to achieve a given degree of polymerization.

$$r = \frac{DP - 1}{DP + 1} \quad (4)$$

- Targeting a degree of polymerization DP for the final PHU



Scheme S3: Synthesized NIPUs in BMA for solubility studies (10wt% of PHU monomers, $T=80^\circ\text{C}$, 24h reaction)

It is firstly important to mention that under the conditions used, only partial solubility of the monomers could be obtained.

Regarding the diamines, the aliphatic diamines (4DA, 6DA, 10DA, 12DA), which are white powders, were not fully soluble after pre-heating during 30 min (time at which the bisCC was added). After adding bisCC-C₁₀, the reactions were left at 80°C to react during 24h to see whether the polymerization would occur by progressive consumption of the monomers (note that bisCC-C₁₀ is soluble in these conditions after 30 min at 80°C in BMA).

After reaction, the vials were removed from the oil bath and the solubility of the resulting polymer was checked. Table S1 summarizes the results and Figure S8 displays pictures of the vials in the case in which bisCC-C₁₀ was copolymerized with different diamines using a stoichiometric ratio of the reactive moieties. As it can be observed, only the formulation involving the branched P1075 led to a soluble polymer at 80°C . The solubility was maintained at room temperature (RT).

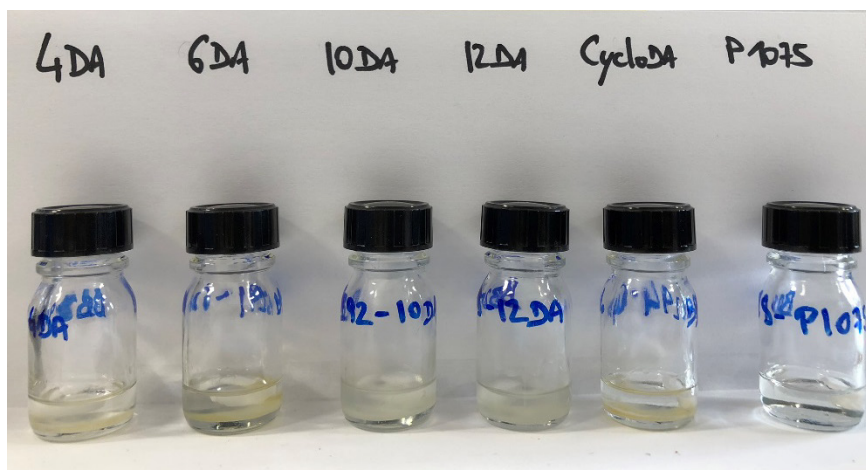


Figure S8: Typical resulting mixtures after PHU formation (10 wt % solids) in BMA

Table S1: PHU solubilities in BMA depending on their chemical structures and targeted DPs (10 wt.% PHU, 24h reaction, T = 80°C)

	bisCC-C ₁₀		
	Targeted DP 2	Targeted DP 5	Targeted DP ∞
4DA	X	X	X
6DA	X	X	X
10DA	X	X	X
12DA	X	X	X
CycloDA	X	X	X
P1075	✓	✓	✓

✓ : soluble

X : not soluble

The reason for the solubility of the PHUs from P1075 may be due to the branched structure of this monomer that bring very high flexibility to the resulting PHU.

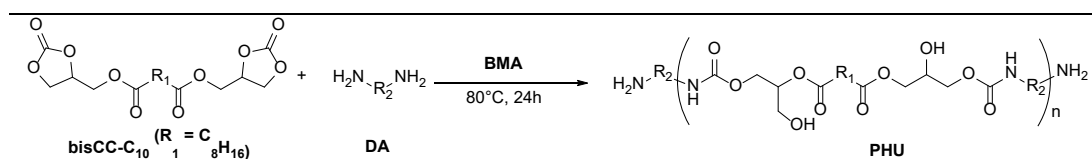
Regarding the other formulations, none of them yielded a soluble product, whatever the targeted polymer structure or targeted degree of polymerization. No further characterization was undertaken because those products could not be of use for the formation of PHU-(meth)acrylic hybrids.

Building upon those outcomes, it appeared quite clear that the introduction of a branched structure was essential in order to achieve solubility of the PHU in BMA, necessary condition for the synthesis of H-NIPUs.

‘Classical’ polyurethanes are segmented materials that are nano-phase segregated. This is done by copolymerizing altogether hard and soft segments (namely short and long comonomers). As a consequence, the introduction of aliphatic segments in the PHU formulation could be of interest in order to access H-NIPU of various properties.

Different PHU structures were targeted by copolymerization of bisCC-C₁₀ with different ratios of 4DA, 10DA and P1075. In all the cases, the total concentration of PHU was 10 wt% and stoichiometric ratio of the reactive moieties was used. Table S2 summarizes these PHUs and their solubility in BMA at 80°C right after reaction and after cooling at room temperature.

Table S2: Effect of chemical composition on the solubility of PHU copolymers in BMA (10wt% PHU, Targeted stoichiometric ratio of the reactive moieties, 24h, T = 80°C)



Ref	PHU		PHU	
	Aliphatic DA	P1075 ^a	Soluble at RT	Soluble at 80°C
1	4DA	0%	X	X
2	4DA	25%	X	X
3	4DA	50%	X	X
4	4DA	75%	X	✓
5		100%	✓	✓
6	10DA	0%	X	X
7	10DA	25%	X	X
8	10DA	50%	X	✓
9	10DA	75%	X	✓
10		100%	✓	✓

✓ : soluble

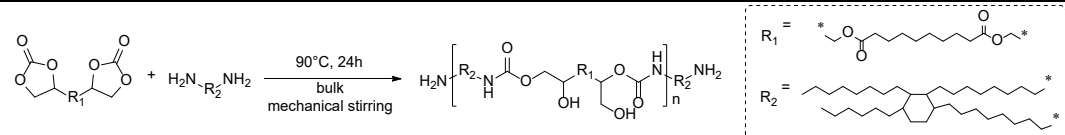
X : not soluble

^a the molar fraction of P1075 is provided as percentage of the total amount of diamine that has to be added for the stoichiometric ratio to be respected

Table S2 shows that at least 75 mol% of P1075 is necessary for the PHU to be soluble in BMA at 80°C. It could also be noticed that the length of the aliphatic diamine had almost no effect.

The solubility experiments detailed above were restricted to 10 wt%. However, in many cases, higher concentrations of PHU may be desired. Therefore, the solubility of PHU synthesized by reacting bisCC-C₁₀ with P1075 in bulk was determined. To do so, the monomers were added in stoichiometric amounts in a Schlenk vessel and left under mechanical stirring at 90°C during 24h. The resulting PHU were then incorporated into BMA and left under magnetic stirring for 1h. The results are presented in Table S3.

Table S3: Solubility of the PHU (made of stoichiometric amounts of bisCC-C₁₀ and P1075) in BMA as a function of the concentration and temperature



Concentration (PHU/BMA)	50wt%			40wt%	
	80°C	40°C	RT	40°C	RT
Solubility	✓	✗	✗	✓	✗

✓ : soluble
 ✗ : not soluble

Interestingly, it can be noticed that high concentrations of PHU in BMA could be reached in this way. Up to 50 wt% of PHU could be solubilized provided the temperature was high enough (80°C in this case).

3. Study on thermal initiation

3.1. Formulations

Table S4: Formulation used in the Run S1 to Run S6.

Reference		S1		S2		S3		S4		S5		S6	
N2-flushing Time		40 min		40 min		25 min		30 min		25 min		20 min	
		Before Initiation	After Initiation										
Basic recipe	PHU	0.961 g		0.947 g	0.820 g	0.820 g		0.966 g		0.887 g		0.844 g	
	(/PHU+BMA) wt%	10.0	9.0	10.0	10.0	10.0	8.7	10.0	9.1	10.0	9.0	10.0	9.2
	BMA	8.652 g		8.526 g	7.376 g	7.376 g		8.670 g		7.965 g		7.585 g	
	(/PHU+BMA) wt%	90.0	91.0	90.0	90.0	90.0	91.3	90.0	90.9	90.0	90.9	90.0	90.8
	MAAc									0.104 g			
	wbo wt%									1.12	1.01		
	SA	0.401 g		0.395 g	0.342 g	0.342 g		0.402 g		0.369 g		0.352 g	
wbo wt%	4.0	3.63	4.0	4.0	4.0	3.49	4.0	3.64	4.0	3.58	4.0	3.71	
Post Stabilization	Dowfax™ 2A1	0.100 g		0.101 g	0.100 g	0.100 g		0.100 g		0.100 g		0.099 g	
	wbo wt%	1.00	0.91	1.02	1.17	1.17	1.02	1.00	0.91	1.07	0.97	1.13	1.05
	Water	9.897 g		9.904 g	9.901 g	9.901 g		9.903 g		9.898 g		14.901 g	
Initiation	Dowfax™ 2A1	0.100 g		0.099 g	0.100 g	0.100 g		0.201 g		0.100 g		0.100 g	
	wbo wt%	1.00	0.91	1.01	1.18	1.18	1.03	2.00	1.82	1.08	0.97	1.14	1.05
	Water	0.832 g		0.835 g	0.857 g	0.857 g		1.283 g		0.843 g		0.965 g	
Initiation	BPO		0.045 g				0.043 g		0.043 g		0.043 g		0.043 g
	(/BMA+SA) wt%		0.46				0.48		0.43		0.46		0.39
	BMA		1.040 g				1.248 g		1.001 g		0.709 g		1.004 g
TOTAL		22.028 g		21.838 g		22.028 g		22.569 g		25.588 g		21.314 g	
Solid Content (wt%)		51.3		50.8		51.3		50.4		49.6		38.0	

3.2. Results & Discussion

Table S5 summarizes the experiments carried out using the thermal initiators (benzoyl peroxide, BPO and azobisisobutyronitrile, AIBN). In all cases, the initiators were added as a shot, after the miniemulsion prepared by sonication had been flushed with nitrogen and equilibrated at a temperature of 70°C. These initiators were not incorporated to the organic phase prior the formation of the miniemulsion because miniemulsification was carried out at 80°C to enhance the solubility of PHU in the monomers. At this temperature, both initiators decompose forming radicals that would initiate polymerization. BPO and AIBN were solubilized in a small amount of neat BMA, as described in the formulations below. The targeted solids content was 50 wt.%, with a NIPU content of 10 wt.%, based on monomers. After adding the initiator, regular sampling was performed in order to monitor the conversion (by gravimetry) as well as the evolution of the particle size, polydispersity index (PDI) and number of particles (by DLS).

Table S5: Miniemulsion polymerizations carried out using thermal radical initiators

Ref.	Solid Content [wt%]	% PHU [wt%]	Initiator (wt%)	Post-Stab. [wt%]	Meth. Acid [wt%]	Reaction Time [h]	Conv. ^a [%]	Coagulation ^a [wt%]	Particle Size ^b [nm]
S1	51.3	10	BPO (0.5)	1	-	5h30	45	0	195
S2	50.8	10	AIBN (0.5)	1	-	5h30	>99	31	170
S3	51.3	10	AIBN (0.5)	1	-	1h30	>99	12.7	155
S4	50.4	10	AIBN (0.5)	2	-	1h30	>99	12.2	150
S5	49.6	10	AIBN (0.5)	1	1	1h30	>99	21.9	148
S6	38.0	10	AIBN (0.5)	1	-	3h	>99	2.1	130

^a Measured by gravimetry

^b Determined by DLS

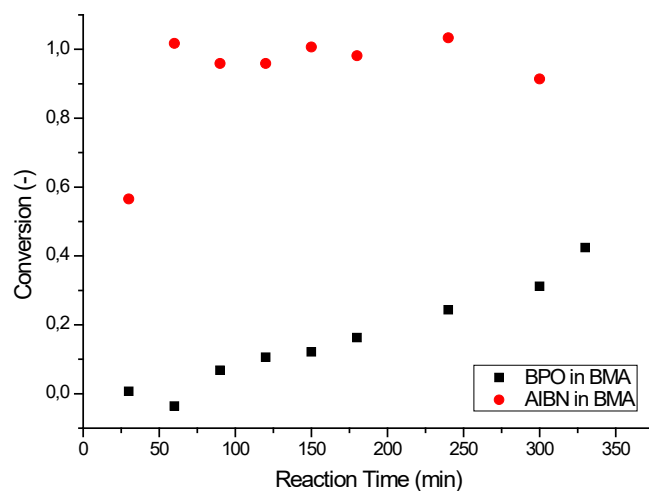


Figure S9: Conversion of BMA obtained by gravimetry upon polymerization with different radical initiators (BPO, run S1; AIBN, run S2). NIPU content: 10 wt.%. Solid content: 50 wt.%.

Figure S9 shows that the polymerization carried out with BPO presented a long inhibition period and only reached 45% after 5.5 hours. This is likely due to the difficulties encountered by the very hydrophobic BPO to reach the miniemulsion droplets/particles; likely as it was added as a shot. This hypothesis is supported by the large particle size obtained with this initiator. The oil soluble AIBN reached complete conversion in less than 1 hour. The significant solubility of AIBN in water (0.04g/100g H₂O⁸) was the likely reason for the fast transfer of this initiator to the droplets. However, a severe coagulation was observed. Comparison between runs S2 and S3 shows that for AIBN a substantial fraction of the coagulum was formed during the long time in which the latex was kept at the reaction temperature (70°C). Attempts to improve the colloidal stability of the dispersion were carried out by increasing the amount of surfactant used in the post-stabilization (run S4) and by using methacrylic acid (MAA) in the formulation (run S5). MAA is highly hydrophilic and upon polymerization tends to concentrate on the surface of the particles, increasing the colloidal stability. However, although the reactions proceed fast (Figure S10), no improvement in colloidal stability was observed.

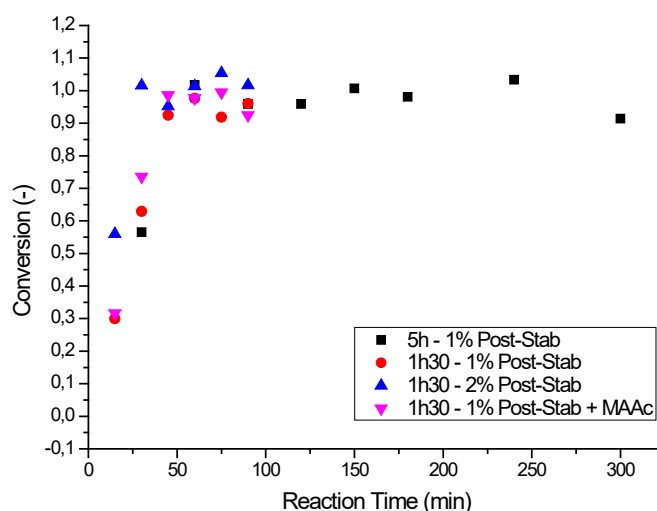


Figure S10: Evolution of the BMA conversion in runs S3-5. PHU content: 10 wt.%. Solid content: 50 wt.%.

Coagulation is a second order process of the number of particles, and hence strongly dependent on the solid content (for similar particle sizes). A reaction using about 40wt% solid was carried out using AIBN, and coagulum was reduced to 2.1%, which is an acceptable value for a lab-scale reactor that often gives higher coagulum fractions than the industrial reactors because of the higher internal surface area (agitator reactor wall)/volume and air interfacial area/volume ratios. Although this is a promising result, because of the uncertainties associated to the distribution of the initiator in large reactors, a redox initiator system (tert-butyl hydroperoxide/ascorbic acid, TBHP/AsAc) was used.

4. Second strategy: Bulk formation of the PHU prior to incorporation into a (meth)acrylic solvent

4.1. Formulations with redox initiators

For feeding purposes, aqueous solutions of TBHP (0.0157 g.mL⁻¹) and AsAc (0.0151 g.mL⁻¹) solution were prepared.

Table S6: Formulations used in the series containing 0, 10, 20 and 30 wt % NIPU (based on the mixture PHU + BMA)

		0 wt% PHU			10 wt% PHU			20 wt% PHU			30 wt% PHU		
N2-Flushing Time		40 min	35 min	25 min	60 min	40 min	35 min	60 min	60 min	60 min	60 min	90 min	45 min
Feeding Time		2h	2h30	3h	2h	2h30	3h	2h	2h30	3h	2h	2h30	3h
Basic recipe	PHU	0 g	0 g	0 g	0.768 g	1.163 g	0.772 g	2.112 g	3.070 g	2.117 g	2.206 g	3.354 g	2.162 g
	<i>(/PHU+BMA) wt%</i>	0	0	0	10.0	10.1	10.0	20.0	20.0	20.0	30.0	30.0	30.0
	BMA	7.709 g	11.519 g	7.585 g	6.914 g	10.369 g	6.953 g	8.427 g	12.309 g	8.444 g	5.152 g	7.831 g	5.048 g
	<i>(/PHU+BMA) wt%</i>	100	100	100.0	90.0	89.9	90.0	80.0	80.0	80.0	70.0	70.0	70.0
	SA	0.321 g	0.480 g	0.316 g	0.320 g	0.481 g	0.322 g	0.439 g	0.640 g	0.440 g	0.307 g	0.466 g	0.301 g
	<i>wbo</i>	4.0	4.0	4.0	4.0	4.0	4.0	4.0	4.0	4.0	4.0	4.0	4.0
	Dowfax™ 2A1	0.080 g	0.120 g	0.079 g	0.080 g	0.120 g	0.080 g	0.110 g	0.160 g	0.110 g	0.076 g	0.116 g	0.075 g
<i>wbo wt%</i>	1.00	1.00	0.99	1.00	1.00	0.99	1.00	1.00	1.00	0.99	1.00	1.00	
	Water	11.923 g	17.881 g	11.773 g	11.927 g	17.881 g	11.924 g	16.397 g	23.853 g	16.387 g	11.327 g	17.370 g	11.177 g
Post Stabilization	Dowfax™ 2A1	0.081 g	0.119 g	0.079 g	0.081 g	0.120 g	0.081 g	0.105 g	0.160 g	0.111 g	0.077 g	0.117 g	0.075 g
	<i>wbo wt%</i>	1.00	0.99	1.00	1.01	1.00	1.00	0.96	1.00	1.00	1.01	1.00	1.00
	Water	0.595 g	0.648 g	0.545 g	0.695 g	0.766 g	0.670 g	0.638 g	1.101 g	0.650 g	0.620 g	0.851 g	0.677 g
Initiation	TBHP	0.0038 g	0.0057 g	0.0038 g	0.0038 g	0.0058 g	0.0038 g	0.0042 g	0.0077 g	0.0042 g	0.0038 g	0.0049 g	0.0038 g
	<i>(/BMA+SA) wt%</i>	0.05	0.05	0.05	0.05	0.05	0.05	0.05	0.06	0.05	0.07	0.06	0.07
	AsAc	0.0037 g	0.0056 g	0.0037 g	0.0037 g	0.0056 g	0.0037 g	0.0041 g	0.0075 g	0.0041 g	0.0037 g	0.0048 g	0.0037 g
	<i>(/BMA+SA) wt%</i>	0.05	0.05	0.05	0.05	0.05	0.05	0.05	0.06	0.05	0.07	0.06	0.07
	Water	0.492 g	0.734 g	0.492 g	0.492 g	0.739 g	0.492 g	0.542 g	0.985 g	0.542 g	0.492 g	0.630 g	0.492 g
TOTAL		21.209 g	31.512 g	20.877 g	21.280 g	31.650 g	21.302 g	28.778 g	42.293 g	28.809 g	20.265 g	30.745 g	20.015 g
Solid Content (wt%)		37.9	37.2	37.0	37.6	38.0	37.8	38.1	37.9	38.1	38.8	37.9	38.5

4.2. SEC-MALLS Traces

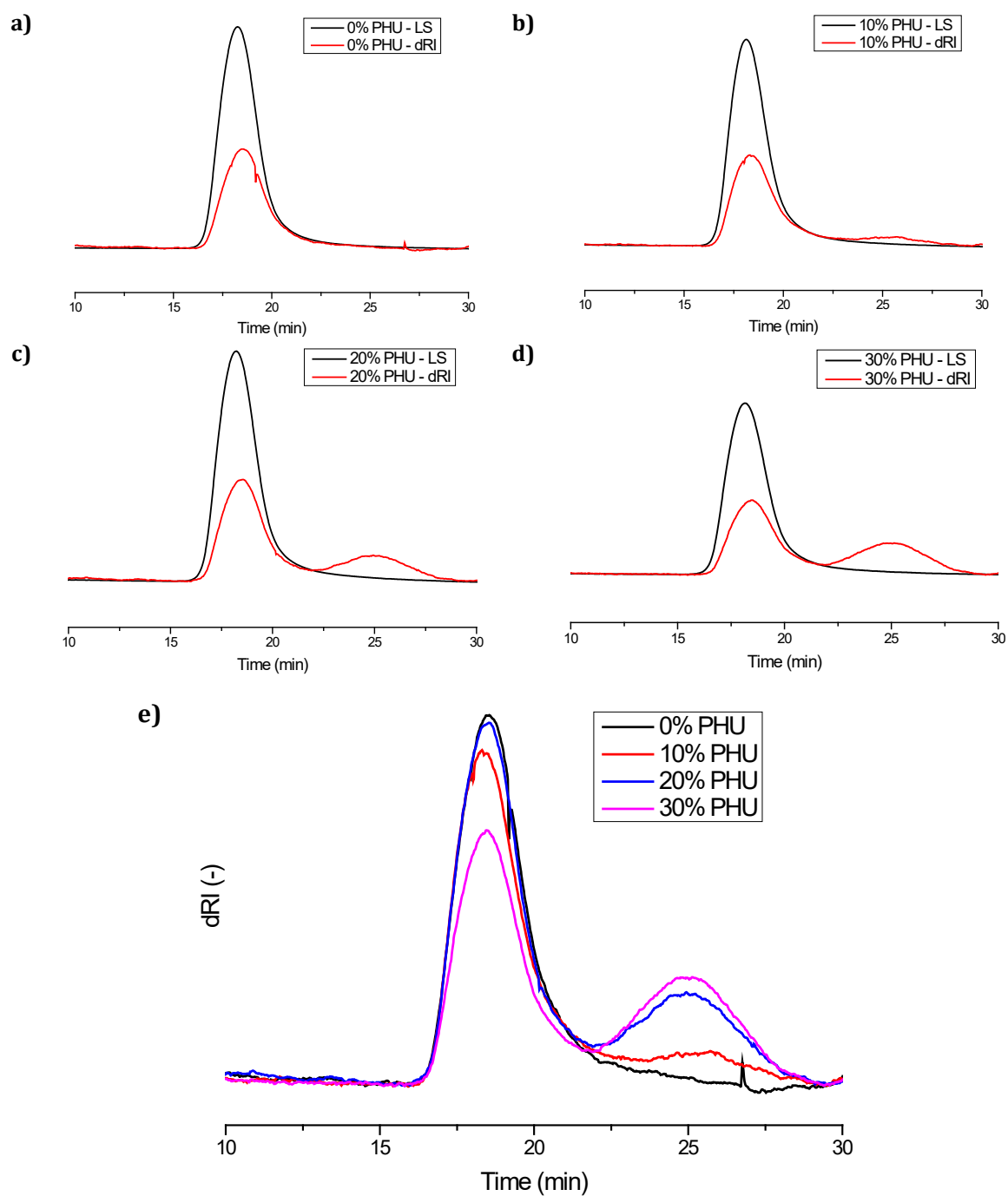


Figure S11: SEC-MALLS traces of the hybrids containing a) 0 % PHU, b) 10 wt.% PHU, c) 20 wt.% PHU and d) 30 wt.% PHU. e) provides the stacked traces obtained from the refractive index signal for hybrids containing 0% to 30 wt.% PHU

4.3. DSC Traces

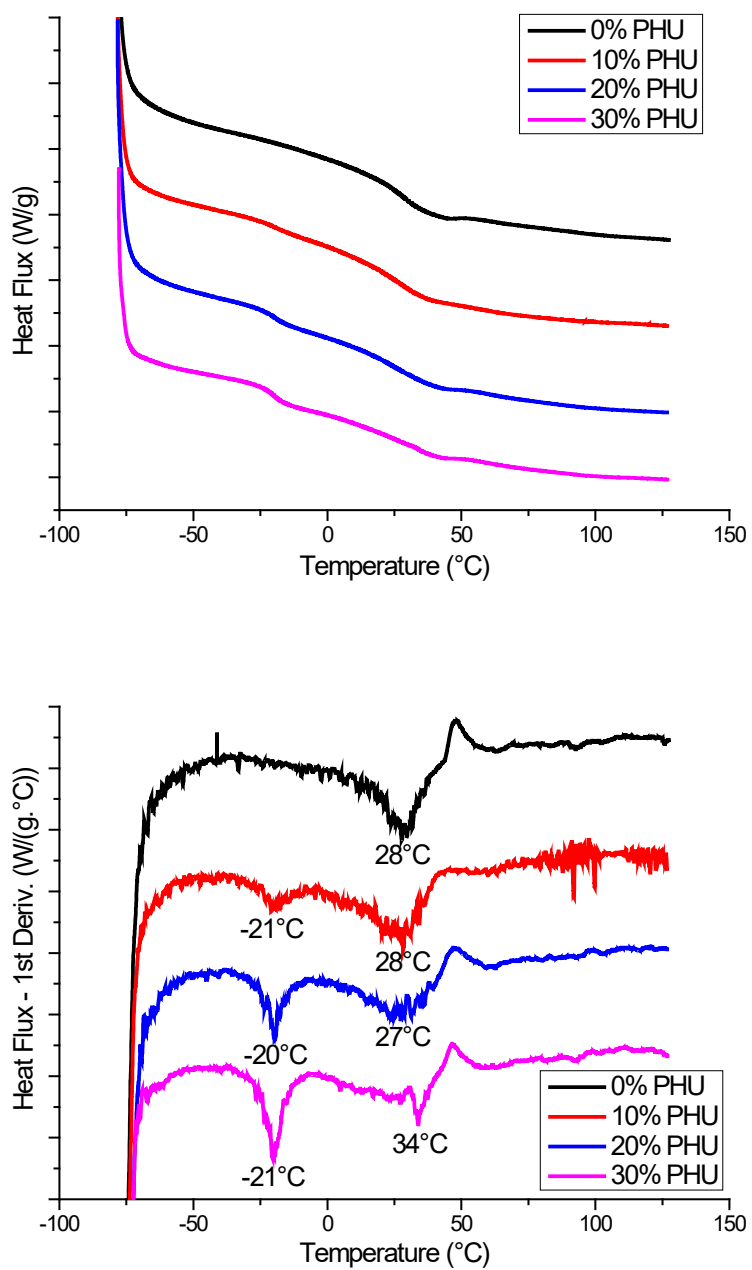


Figure S12: DSC traces (top) and first derivative of the DSC traces (bottom) of the films cast from the latexes fed during 2h30 with AsAc – 1st heating ramp (10°C.min⁻¹)

4.4. Minimum Film Forming Temperature (MFFT)

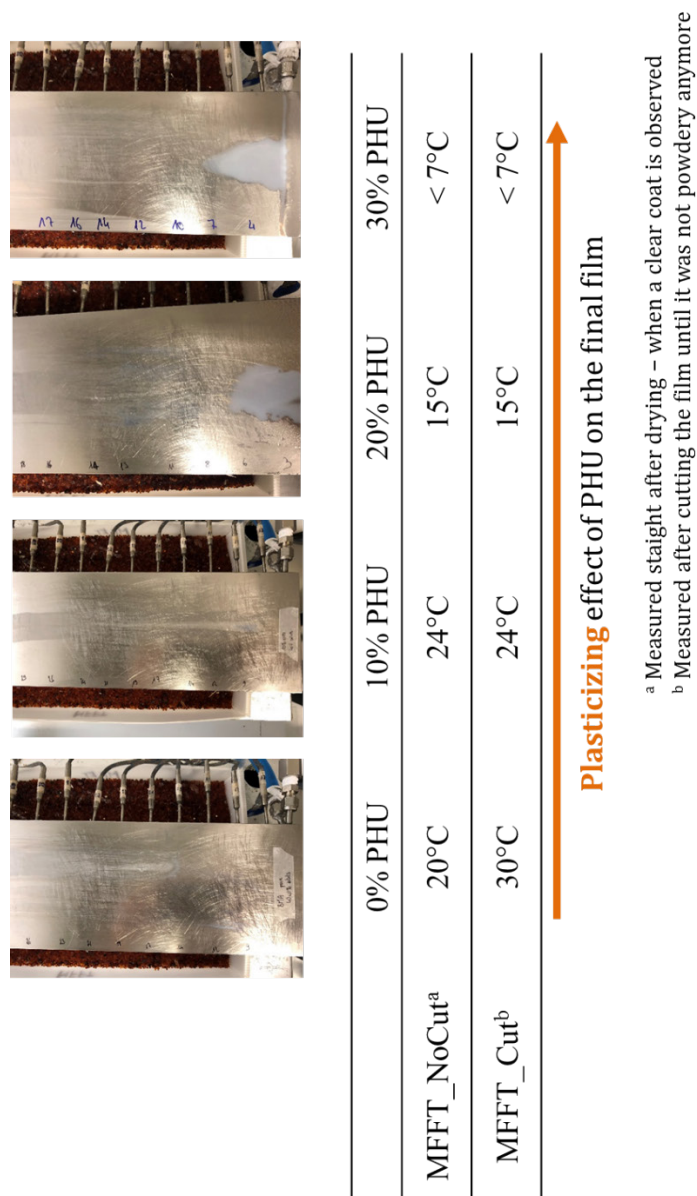


Figure S13: Measurement of the MFFT of the latexes fed during 2h30 with AsAc

5. References

- (1) Rix, E.; Grau, E.; Chollet, G.; Cramail, H. Synthesis of Fatty Acid-Based Non-Isocyanate Polyurethanes, NIPUs, in Bulk and Mini-Emulsion. *Eur. Polym. J.* **2016**, *84*, 863–872.
- (2) Lamarzelle, O.; Durand, P.-L.; Wirotius, A.-L.; Chollet, G.; Grau, E.; Cramail, H. Activated Lipidic Cyclic Carbonates for Non-Isocyanate Polyurethane Synthesis. *Polym. Chem.* **2016**, *7*, 1439–1451.
- (3) Bassam, N.; Laure, C.; Jean-François, B.; Yann, R.; Zephirin, M. Aza-Michael versus

Aminolysis Reactions of Glycerol Carbonate Acrylate. *Green Chem.* **2013**, *15* (7), 1900–1909.

- (4) Cornille, A.; Ecochard, Y.; Blain, M.; Boutevin, B.; Caillol, S. Synthesis of Hybrid Polyhydroxyurethanes by Michael Addition. *Eur. Polym. J.* **2017**, *96*, 370–382.
- (5) Schimpf, V.; Asmacher, A.; Fuchs, A.; Bruchmann, B.; Mülhaupt, R. Polyfunctional Acrylic Non-Isocyanate Hydroxyurethanes as Photocurable Thermosets for 3D Printing. *Macromolecules* **2019**, *52* (9), 3288–3297.
- (6) Morinaga, H.; Morikawa, H.; Sudo, A.; Endo, T. A New Water-Soluble Branched Poly(Ethylene Imine) Derivative Having Hydrolyzable Imidazolidine Moieties and Its Application to Long-Lasting Release of Aldehyde. *J. Polym. Sci. Part A Polym. Chem.* **2010**, *48* (20), 4529–4536.
- (7) Odian, G. Step Polymerization. In *Principles of Polymerization*; John Wiley & Sons, Inc., 2004; pp 39–197.
- (8) Alduncin, J. A.; Forcada, J.; José, A. Miniemulsion Polymerization Using Oil-Soluble Initiators. *Macromolecules* **1994**, *27* (8), 2256–2261.